JOURNAL OF QUATERNARY SCIENCE (2023) 1–18 ISSN 0267-8179. DOI: 10.1002/jqs.3587

JQS Journal of Quaternary Science QRA Quaternary Research Association

Influence of flooding variability on the development of an Amazonian peatland

D. SASSOON,[1,2]* W. J. FLETCHER,[1] K. H. ROUCOUX,[3] P. RYAN,[1] I. T. LAWSON,[3] E. N. HONORIO CORONADO,[3] J. DEL AGUILA PASQUEL,[4] T. BISHOP,[1] C. M. ÅKESSON[3] and A. HASTIE[5,6]

[1]Quaternary Environments and Geoarchaeology Research Group, Department of Geography, University of Manchester, Manchester, UK
[2]Muséum national d'Histoire naturelle, UMR 7194 Histoire Naturelle de l'Homme Préhistorique, Paris, France
[3]School of Geography and Sustainable Development, University of St Andrews, St Andrews, UK
[4]Instituto de Investigaciones de la Amazonía Peruana, Iquitos, Peru
[5]Carbon and Wetlands Group, Faculty of Science, Charles University, Prague, Czech Republic
[6]School of GeoSciences, University of Edinburgh, Edinburgh, UK

Received 14 April 2023; Revised 25 October 2023; Accepted 5 December 2023

ABSTRACT: Peat in the Pastaza–Marañón Foreland Basin (PMFB), northern Peru, forms beneath open wetlands, palm swamps, pole forests and seasonally flooded forests. These vegetation communities may represent different successional stages of peatlands, but the spatiotemporal patterns of peatland development in Amazonia are still poorly understood. We present a new geochemical and palaeoecological record spanning the last c. 4330 years from an open peatland (San Roque, core SAR_T3_03_B). Our results suggest the persistence of predominantly herbaceous vegetation communities at the core site since the start of peat accumulation (c. 3180 cal a BP). Micro-X-ray fluorescence core scanning provides evidence for episodes of fluvially derived minerogenic input and simultaneous increases in flood-tolerant taxa relating to intervals of increased frequency and depth of riverine flooding. The establishment of *Mauritia flexuosa* palms from around 440 cal a BP coincided with a shift to lower flooding depth and frequency which continues to the present day. This study reveals the role of flooding variability in shaping peatland development and influencing vegetation succession in the PMFB, underlining the need to understand natural environmental variability for the conservation of these ecosystems due to their vital contributions to ecosystem services and carbon storage. © 2023 The Authors *Journal of Quaternary Science* Published by John Wiley & Sons, Ltd

KEYWORDS: Amazonia; flooding; palynology; peatlands; vegetation dynamics

Introduction

Recent research in Amazonian lowland peatlands has highlighted the significance of river proximity, flood duration and flood depth as pivotal factors influencing peatland ecosystems (Roucoux et al., 2013; Lawson et al., 2014; Kelly et al., 2017, 2020). Recent climate model projections for Amazonia predict an intensification of the hydrological cycle and enhanced seasonality leading to increased severity of both floods and droughts by 2100 (e.g. Cox et al., 2004; Malhi et al., 2009; Gloor et al., 2013), so it is critically important to understand how peatlands respond to such changes. These ecosystems provide vital services, such as contributing to below-ground carbon storage, adding to regional biodiversity (Page et al., 2011; Draper et al., 2018; Honorio Coronado et al., 2021), and providing habitats for threatened animal species (Gilmore et al., 2013; Bodmer et al., 2018), as well as benefitting human communities and the local economy (Roucoux et al., 2017; Schulz et al., 2019). Changes to hydrological dynamics in response to climate change threaten the delicate balance that drives peat formation, vegetation succession, nutrient content, carbon sequestration and decomposition processes (Ribeiro et al., 2021). In this context, palaeoecological records offer a unique opportunity to evaluate 'natural experiments' to investigate the variability of flooding regimes and their impact on long-term peatland development and successional changes. This approach represents an important contribution to the evidence base that enables us to predict future changes and thereby understand the best approach to conserve tropical peatlands.

The Pastaza–Marañon Foreland Basin (PMFB), situated in the Loreto Department in northeast Peru, hosts the largest peatland area in Amazonia, most of which is hydrologically intact (Schulman et al., 1999; Freitas Alvarado et al., 2006; Lähteenoja et al., 2009a, b; Draper et al., 2014; Hastie et al., 2022). Within this region, four ecosystem types associated with peat have been identified, namely peatland palm swamps, peatland pole forests, open peatlands and occasionally seasonally flooded forests (Lähteenoja and Page, 2011; Flores Llampazo et al., 2022). Although these ecosystem types are floristically distinct in the PMFB (Draper et al., 2018; Honorio Coronado et al., 2021; Hastie et al., 2022), recent fieldwork and palynological investigations have revealed a range of intermediate ecosystems, suggesting greater complexity of peatland ecosystems and environments than had previously been appreciated.

Previous work on the palaeoenvironmental history of the Quistococha palm swamp and the San Jorge pole forest (Figure 1) has revealed characteristic successional pathways

*Correspondence: D. Sassoon, as above.
Email: dael.sassoon@gmail.com

involving the different ecosystem types during the formation and development of the peatlands. Both records suggest that the shift from inorganic material to peat was linked to reduced sediment input due to changes in the river's course (Roucoux et al., 2013; Kelly et al., 2017). Vegetation at Quistococha evolved from a herbaceous wetland to a seasonally flooded forest and ultimately to a palm swamp over about 1000 years, while San Jorge followed a similar pattern from herbaceous fen to palm swamp (but lacked a seasonally flooded forest phase), eventually transitioning to present-day pole forest vegetation around 200 years ago (Roucoux et al., 2013; Kelly et al., 2017, 2020). At both sites, the shift towards a palm swamp, dominated by the *Mauritia flexuosa* palm, was attributed to changes in the flooding regime. This involved a shift from deep seasonal flooding (3–5 m), unsuitable for *Mauritia flexuosa* due to its intolerance to flooding above 1.2 m, to permanently waterlogged conditions with less frequent and/or shallower seasonal floods tolerated by *Mauritia flexuosa* (Junk et al., 2015; Flores Llampazo et al., 2022). Based on what is known about peatland terrestrialization and the possible patterns of ecological succession from lake to bog after foundational work by Walker (1970), the records at Quistococha and San Jorge match the 'expected' pathways of succession from open water to closed forest. However, Draper's (2015) work on the open peatland of Veinte de Enero and the pole forest of Ollanta revealed that not all peatlands follow the same spatiotemporal pattern of terrestrialization and that vegetation can remain open (i.e. without a closed-canopy forest) for hundreds to thousands of years. Kelly et al. (2017) also noted the effect of allogenic factors on peatland vegetation succession, and suggested that the occurrence of wetter phases, driven either by climatic or hydrological processes or a combination of the two, can interrupt the process of terrestrialization.

From the above studies, proximity to the river and changes in flooding emerge as key drivers of change in peatland ecosystems. This is consistent with early observations by Puhakka et al. (1992), who pointed out that patches of successional forests often occur along laterally migrating rivers in the Peruvian Amazon, and their distribution and succession are determined by the changes in river dynamics. It is our working hypothesis that differences in spatiotemporal succession between peatlands in the PMFB – some of which undergo rapid succession (over a few thousand years), while others seem to not to progress for prolonged intervals of time – may be regulated by the variability of the flooding regime. This study represents a necessary investigation into open herbaceous peatlands in Amazonia to understand their relationship with other peatland types, combining palynology and geochemistry in order to analyse the influence of flooding variability on peatland development in more detail.

Here we present new palaeoecological and geochemical evidence from a peat core sampled close to the community of San Roque, located north of the Marañón river, in the PMFB. The coring site was identified as an 'open peatland' through landcover classification using remotely sensed data (Honorio Coronado et al., 2021) and our field observations confirm the presence of an open canopy. However, there are also abundant scattered trees including the peatland palm swamp specialist *Mauritia flexuosa* and the typical pole forest tree *Pachira* sp., representing an intermediate situation between entirely open, herbaceous peatland, and closed peatland palm swamp or pole forest. This new site thus presents an opportunity to better understand the transitions between different peat-forming vegetation types and the related changes in hydrology.

This study aims to analyse new high-resolution palynological and geochemical data from the San Roque peatland to: (i) reconstruct past vegetation changes; (ii) investigate the interaction between the fluvial system and the peatland's vegetation dynamics over time; and (iii) determine how patterns of ecological and fluvial change at San Roque compare with records from other peatland types in the wider PMFB, to better understand the sensitivity of peatlands to flood regime.

Study area

Regional context

The PMFB, located in the Loreto Department in northeast Peru, comprises around 62 714 km^2 of potential peat-forming vegetation (Hastie et al., 2022). Peatlands in the PMFB represent a globally important carbon store (Schulman et al., 1999; Freitas Alvarado et al., 2006; Lähteenoja et al., 2009a, b), holding an estimated 5.4 Pg of carbon (Hastie et al., 2022), most of which is below-ground in the form of peat – defined as substrates composed of ≥65% organic material and ≥0.3 m thickness (Charman, 2002; Wüst et al., 2003; Lawson et al., 2014; Dargie et al., 2017). Peat in the PMFB can reach 7–8 m in thickness, and basal ages of almost 9000 cal a BP have been reported (Lähteenoja et al., 2012).

Field sampling and floristic assessments have revealed important information about the peatland ecosystems that occur in the PMFB. Peatland palm swamps (*aguajales*) represent the majority of the peatlands in the PMFB (43 338 km^2) and are dominated by the palm *Mauritia flexuosa* L.f. (Arecaceae), with an above-ground carbon (AGC) storage of 75.61 ± 8.44 Mg C ha^{-1}, below-ground carbon (BGC) of 22.50 ± 2.41 Mg C ha^{-1} and soil organic carbon (SOC) of 647.76 ± 80.37 Mg C ha^{-1} (Honorio Coronado et al., 2021). Peatland pole forests (*varrillal hidromorfico*) account for 7540 km^2 and are characterized by low-stature forests with limited diversity and thin-stemmed trees, often harbouring monodominant species such as *Pachira nitida* (Palacios et al., 2016; Draper et al., 2014; López Gonzales et al., 2020), with an AGC of 78.24 ± 13.17 Mg C ha^{-1}, a BGC of 21.18 ± 3.08 Mg C ha^{-1} and SOC of $1{,}033.75 \pm 91.57$ Mg C ha^{-1} (Honorio Coronado et al., 2021). So-called 'open peatlands' (*pantano abierto de turbera*, or *pantano herbaceo-arbustivo*), which are named as such due to their significantly more open canopies compared with peatland palm swamps and pole forests, occupy a comparatively smaller area of 4888 km^2 (Draper et al., 2014; Draper, 2015; Hastie et al., 2022) and have an AGC of 41.26 ± 22.71 Mg C ha^{-1}, a BGC of 15.59 ± 8.72 Mg C ha^{-1} and SOC of 628.27 ± 131.85 Mg C ha^{-1} (Honorio Coronado et al., 2021). More rarely, peat has been found in seasonally flooded forests, specifically in the roughly 2% that maintain a consistently high water table throughout the year (Lähteenoja and Page, 2011; Flores Llampazo et al., 2022; Hastie et al., 2022).

The climate in the study region is hot and humid, with an average annual temperature of 26 °C, a daily minimum of 20–22 °C and a maximum of 29–31 °C (Marengo et al., 1998). Relative humidity averages 80–90% throughout the year (Tafur Rengifo, 2001). Average annual precipitation in Iquitos is 3180 mm (Honorio Coronado et al., 2015). Seasonal variation in precipitation is low, with a wetter season from December to March and a drier season from July to September (Marengo et al., 1998). Flooding in this region is characterized by annual flood pulses during the December–March interval; highest water levels in the Marañón river occur between March and May, and the lowest levels in September (Dumont and Garcia, 1991; Honorio Coronado et al., 2015), with a difference of almost 5 m between low and high water (Lähteenoja et al., 2012). During the wet season, a cumulative area of over 60 000–70 000 km^2 between the Ucayali, Huallaga, Tigre and

Marañón rivers is flooded (Räsänen et al., 1992). Precipitation during the wet season also increases the wetness of the low-lying interfluvial areas which are not directly affected by river flooding, and this causes a hydrological flow of water from the wetlands into the surrounding network of streams and rivers (Mertes, 1997). Water levels in the region are affected by large-scale patterns of interannual climatic variability originating in sea surface temperatures (SSTs) and atmospheric pressure gradients in the tropical Atlantic and Pacific (Gloor et al., 2015). For example, the combined influence of the El Niño Southern Oscillation (ENSO) and changes in North Atlantic SST is thought to contribute to changes in the severity and seasonality of floods and droughts in northwestern Amazonia (Gloor et al., 2015; Marengo et al., 2008; Marengo and Espinoza, 2016).

Study site

The San Roque peatland – informally named after the nearest village (4°28′36″ S, 74°35′26″ W) – covers about 22 km^2 and is located around 250 km upstream from the city of Iquitos on the northern bank of the Marañón river (Figure 1). The location of the peat core site (SAR_T3_03_B) was chosen based on its position close to a large meander of the Marañón river, which means that its development may have been directly influenced by fluvial dynamics (e.g. cut-off channel or oxbow lake), thus providing the potential to test our ideas about how rivers can affect peatland ecosystem development. Peat thickness at the site, as determined by augering, ranged from 30 cm at the edge to 580 cm in the centre. The peatland is permanently water-logged, the water table being at or near the surface year-round, enabling peat to accumulate (Flores Llampazo et al., 2022). At the time of sampling (July 2019), during the end of the wet season, standing water height measured 10–20 cm above the peat surface.

A series of vegetation survey plots, including five 0.1-ha temporary plots (ROQ-01 to ROQ-05; ROQ standing for 'Roque') were established in the area to document the vegetation assemblages around the study's coring site (see the ROQ plots in Figure 1; Honorio Coronado et al., 2021). The San Roque open peatland (shown in blue and cyan in the Landsat mosaic; Figure 1) is bordered by a palm swamp peatland (shown in red) on its southern, eastern and northern–eastern margins, a seasonally flooded forest (shown in orange) to the southwest and pole forest peatland (shown in dark red) to the northwest. The peat core site is located in an area of open peatland characterized by a relative scarcity of trees when compared with the surrounding vegetation (Figure 2). For example, the tree community of the open peatland vegetation plot ROQ-03 is sparse: *Mauritia flexuosa* (20 stems), *Pachira nitida* (3) and *Ficus americana* (1). The pole forest (ROQ-02) is characterized by a community with *Pachira nitida* (69 stems), *Platycarpum loretense* (25) and *Mauritia flexuosa* (4). The seasonally flooded forest (ROQ-05) has higher tree and palm diversity, dominated by *Mauritiella armata* (28), *Vatairea guianensis* (7), *Tabebuia insignis* (6), *Eugenia florida* (6) and another 15 less abundant species (51 stems in total) including *Coussapoa trinervia* and *Symphonia globulifera*. Although no formal surveys were carried out in the peatland palm swamp at San Roque, field observations revealed the dominance of *Mauritia flexuosa*, accompanied by several tree species including *Tabebuia insignis*, *Hevea guianensis* and *Alchorneopsis* sp., similar to *Mauritia flexuosa*-dominated peatland palm swamps studied in detail elsewhere in the PMFB (Roucoux et al., 2013; Honorio Coronado et al., 2021).

Materials and methods

Pollen-vegetation representation

To understand the representation of modern vegetation in the pollen rain, floristic data were collected from a new permanent 0.5-ha (50 × 100-m) forest census plot (ROQ-06), co-located with ROQ-03 (Figure 1). This size of plot is judged to adequately capture the relatively low diversity of peatland ecosystems (Honorio Coronado et al., 2021). Following the RAINFOR protocol (Phillips et al., 2010), all stems ≥10 cm in diameter at breast height (DBH, 1.3 m) and understorey plants (stems 1–9 cm DBH) were recorded. Species were identified using herbarium specimens at the Instituto de Investigaciones de la Amazonía Peruana (IIAP), Iquitos.

To obtain samples of the modern pollen rain, surface samples were collected from two of the temporary 0.1-ha

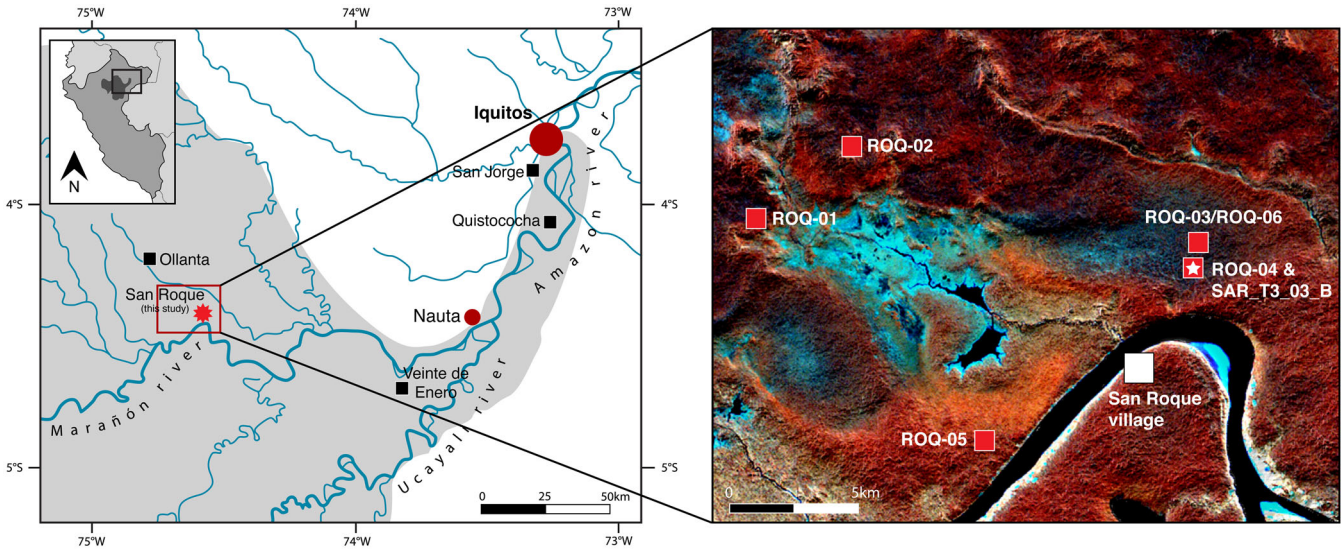

Figure 1. Left: map of the study area, showing the location of major local towns (red circles), the peatland sites relevant to this study (black squares) and the location of the San Roque peatland (red star). The shaded area indicates the extent of the PMFB. Right: remotely sensed map of San Roque showing the coring location (marked by a star) and vegetation plots (red squares), combining Landsat, Palsar and Srtm-30 imagery. Landsat uses bands 3, 2 and 1, assigned to red, green and blue, respectively. Black = rivers and channels; beige = terra firme; orange = seasonally flooded forest; red = palm swamp; maroon = pole forest; blue/cyan = flooded land and open peatlands. [Color figure can be viewed at wileyonlinelibrary.com]

Figure 2. Photos (taken in July 2019) showing the difference between the vegetation structure and canopy of: (A) the San Roque open peatland around the coring site SAR_T3_03_B; (B) the seasonally flooded forest plot at San Roque; (C) the pole forest plot at San Roque; and (D) the palm swamp of Veinte de Enero. [Color figure can be viewed at wileyonlinelibrary.com]

vegetation plots, ROQ-04 and ROQ-03, which are both in open peatland, located 1 and 2 km north of the Marañón river, respectively (Figure 1). Four samples of surface peat were collected in each plot, one from each cardinal corner. After the pollen was extracted and counted (see 'Pollen analysis' below), the pollen spectra of the eight samples were merged and compared with the forest census data from ROQ-06.

Core collection

A 570-cm core (SAR_T3_03_B) was collected using a Russian corer from the open peatland plot ROQ-04 (4°26′39.55″ S, 74°34′7.07″ W). Two parallel boreholes set 1 m apart were used to avoid disturbance of the peat below with the tip of the corer, with an overlap of 10 cm between each core section to ensure continuity of the record (Brown, 2010). Coring continued until underlying inorganic sediment was reached, 20 cm of which was sampled. Samples were transferred from IIAP to the University of St Andrews for storage, and analyses were conducted at the University of Manchester, where they are currently stored under licence at 4 °C.

Sedimentological and geochemical analyses

The core was described using the Troels-Smith (1955) system. To understand lithological variations in the cores arising from varying environmental conditions, volumetric magnetic susceptibility (*K*) of the sediments was measured using a Bartington MS2C loop sensor (Bartington Instruments, UK), at 1-cm intervals (Dearing, 1999). Background *K* was measured at the beginning and end of each core segment to account for drift (Dearing, 1999). Micro-X-ray fluorescence core scanning (μXRF) was implemented to analyse changes in the geochemistry of the sediments (Croudace and Rothwell, 2016). Core sections were loaded in a COX ITRAX μXRF scanner (Cox Analytical Systems, Sweden) at the University of Manchester Geography Laboratories, set to scan each core segment at a 500-μm resolution, using a molybdenum (Mo) target tube at a voltage of 30 kV, and current of 30 mA, with an exposure time of 15 s. Compilation, quality control and visualization of the μXRF elemental data was achieved using R, following the protocols outlined by Bishop (2021). The acceptance criteria for the μXRF data were set at a count rate per second (CPS) of 3000–6000, mean square error (MSE) of <6, sample slope: <100 μm per 500 μm (equivalent to 1/5) and validity = TRUE. Any data points not achieving these criteria were deemed as poor-quality data and excluded. To characterize the organic material in the core, including discrimination of vascular plant and algal sources, carbon/nitrogen (C/N) ratios were measured. Bulk peat samples of 1 cm^3 were taken at 8-cm intervals along the cores and freeze-dried using a Christ Alpha 1-4 LSCplus, ground with an agate pestle and mortar, and homogenized. Three replicates for each sample (weighed to 2 mg using a microbalance) were placed in tin capsules and analysed in a Thermo Flash 2000 elemental analyser operating in CHNS (carbon, nitrogen, hydrogen, sulphur) mode.

Pollen analysis

Subsamples of 1 cm^3 were taken from the peat core at 8-cm intervals, and from the surface samples. Pollen extraction was carried out following standard laboratory techniques (Moore et al., 1991; Faegri and Iversen, 1989), including acetolysis. Clay-rich sediments received additional dense-medium separation using sodium polytungstate (SPT) to remove siliceous material (Campbell et al., 2016). Samples were mounted in silicone oil and examined under a light microscope at ×1000 magnification using immersion oil (Cargille, 2008). For each sample, a target of 500 pollen grains from terrestrial plants was chosen for the main pollen sum, which included trees, shrubs, herbs and grasses and excluded spores (Pteridophytes and algae) and aquatic taxa. This target was chosen to account for the high level of biodiversity in tropical ecosystems compared to temperate regions and to better represent potentially low-pollen-producing taxa such as animal-pollinated plants (Djamali and Cilleros, 2020).

Palynological identification was supported by comparisons with the reference collection at the University of St Andrews, which consists of material gathered from a range of sources including living plants (botanical gardens of Edinburgh and Kew), herbarium specimens (Kew and Jenaro Herrera, Peru) and other pollen reference collections (University of Edinburgh). Reference was also made to pollen descriptions in Colinvaux et al. (2003), Roubik and Moreno (1991) and Absy (1979). The study of Burn and Mayle (2008) was used for identifications within the family Moraceae, and Dias Saba (2007) for the Malvaceae (including *Pachira* and *Ceiba*) and Urticaceae/Moraceae. All pollen morphotypes were identified to the lowest possible taxonomic level. Family-level identifications of pollen taxa were always possible, while genus- or species-level identification was often unachievable. Species-level identification was possible in the following instances: (i) single-species genera; (ii) where other species of the genus are highly unlikely to occur in this environmental setting or geographical region [e.g. *Iriatea deltoidea* (only two species, the other is not yet known in Peru), *Euterpe precatoria* (three species, the other two are only known in white sand forest and cloud forest respectively); Pennington et al., 2004]; and (iii) where pollen morphology is unmistakable [which can combine with conditions above, e.g. *Symphonia globulifera*). Pollen grains identified only to family level are denoted undiff[erentiated].', e.g. 'Poaceae undiff.' where further taxonomic subdivision has not been possible. Pollen 'types' (indicated by a lowercase 't') are morphologically indistinguishable from each other and named after their most likely taxonomic affiliation; for example, '*Cecropia*-t.' includes pollen that is morphologically indistinguishable from the pollen of the genus *Cecropia* and may include pollen produced by other genera (Roucoux et al., 2013). In general, we aimed for consistency in taxonomy with previous studies (i.e. Roucoux et al., 2013; Kelly et al., 2017, 2020). *Mauritia*-t. includes pollen produced by the palm genera *Mauritia* and *Mauritiella* because the genus of individual grains cannot easily be identified based on their morphology alone. However, they can be tentatively distinguished by grain diameter since most grains of *Mauritia* are larger than 40 µm, and most grains of *Mauritiella* are smaller than 40 µm, with only a small overlap in grain diameter between the two statistical populations (Kelly 2015). The most likely species in this environmental setting and in this region of Peru are *Mauritia flexuosa* and *Mauritiella armata*, which are important ecological indicators since they tolerate different flooding regimes (Seubert, 1996; Endress et al., 2013; Junk et al., 2015; Kelly et al., 2017). To estimate the relative abundance of these two palm species in the pollen samples, measurements were conducted using image analysis in *ImageJ* (Rasband 2018) and were performed on up to 50 *Mauritia*-t. grains for each of the 18 samples in which this taxon was most abundant. Pollen samples in this study were prepared using the same methodology as in Kelly (2015) (samples were dehydrated using tert-butyl alcohol and preserved in silicone oil, both chemical treatments which can affect pollen grain diameter in the final residues) so that the same size threshold could be used to distinguish the species. Pollen diagrams were created using the *Rioja* 1.0 package (Juggins, 2020) in R 4.1.0 (R Core Team, 2021).

Microcharcoal fragments larger than 5 µm (Kelly, 2015) and palm phytoliths – siliceous particles produced by the leaves (Patterson et al., 1987; Huisman et al., 2018) – appearing in the slides were also counted to provide information about fire history and additional evidence for changes in palm abundance respectively. Although charcoal counts from pollen slides can be artificially high due to particle fragmentation, each sample was treated in the same way and thus the counts can be interpreted as changes in relative charcoal abundance between samples.

Radiocarbon dating

Five samples for radiocarbon dating were taken at approximately equal intervals through the core. Bulk peat samples (5–7 g wet weight) were passed through a 180-µm sieve to remove any non-contemporaneous roots and thus minimize the potential for contamination by modern carbon (Piotrowska et al., 2011; Kelly et al., 2020). The <180-µm bulk peat fine particulate fraction was freeze-dried and samples of 200–500 mg were sent to the Environmental Radiocarbon Laboratory in East Kilbride, Glasgow, for radiocarbon dating by accelerator mass spectrometry (AMS). The age–depth model was constructed using the R package *CLAM* 2.5 (Blaauw, 2010), using a smoothing spline for interpolation. Mixed calibration curves using IntCal20 (Reimer et al., 2020) and SHCal20 (Hogg et al., 2020) (50:50 ratio) were necessary because the study area is located within the Intertropical Convergence Zone (ITCZ; Hogg et al., 2020). Calibration was achieved with the function *mix.curves*, and dates are presented using 95.4% confidence intervals (2σ).

Statistical analyses

The pollen diagram was zoned using Constrained Incremental Sum-of-Squares (CONISS) cluster analysis (Grimm, 1987), based on the abundance of taxa in the main pollen sum. Zonation was undertaken to identify intervals characterized by similar pollen assemblages, and thereby aid the description and interpretation of the results (Birks, 1996).

Results

Comparison of vegetation and modern pollen data

Seven tree species with a DBH ≥ 10 cm are recorded in the 0.5-ha plot ROQ-06 (Supporting Information Appendix S1). In order of abundance (% stems), these are: *Mauritia flexuosa* (82%), *Pachira nitida* (7.5%), *Clusia insignis* (6%), *Tapirira guianensis* (2%), *Ficus guianensis* (2%), *Guatteria guianensis* (1%) and *Pagamea guianensis* (1%). The understorey (stems DBH 1–9 cm) consists of 28 taxa of shrubs, treelets and tree saplings; the six most abundant taxa are: *Matayba inelegans* (70%), *Tapirira guianensis* (64%), *Pachira nitida* (32%), *Tabebuia guianensis* (22%), *Pagamea guianensis* (8%) and *Cybianthus spicatus* (8%). This vegetation assemblage, characterized by scattered *Mauritia flexuosa* palms and an understorey with some thin and short treelets, is intermediate between peatland vegetation types used thus far in peatland carbon and landcover mapping (e.g. Draper et al., 2014; Honorio Coronado et al., 2021; Hastie et al., 2022) since it has elements of entirely 'open', herbaceous peatlands with little to no canopy, as well as (though few in number) trees and palms typical of peatland palm swamp and peatland pole forest. It resembles ecosystems identified by the local Urarina indigenous group as '*jiiri*' which appears to include a range of peatland ecosystems along a gradient of openness from herbaceous peatlands, to herbaceous peatlands with scattered *Mauritia flexuosa*, to very low-stature peatland pole forest (Schulz et al., 2019).

Figure 3 shows the taxa recorded in the surface samples and in the vegetation survey plot (see also Appendix S2). The tree taxa >10 cm DBH recorded in the plots that were not observed in the surface samples are *Clusia insignis*, *Guatteria guianensis*

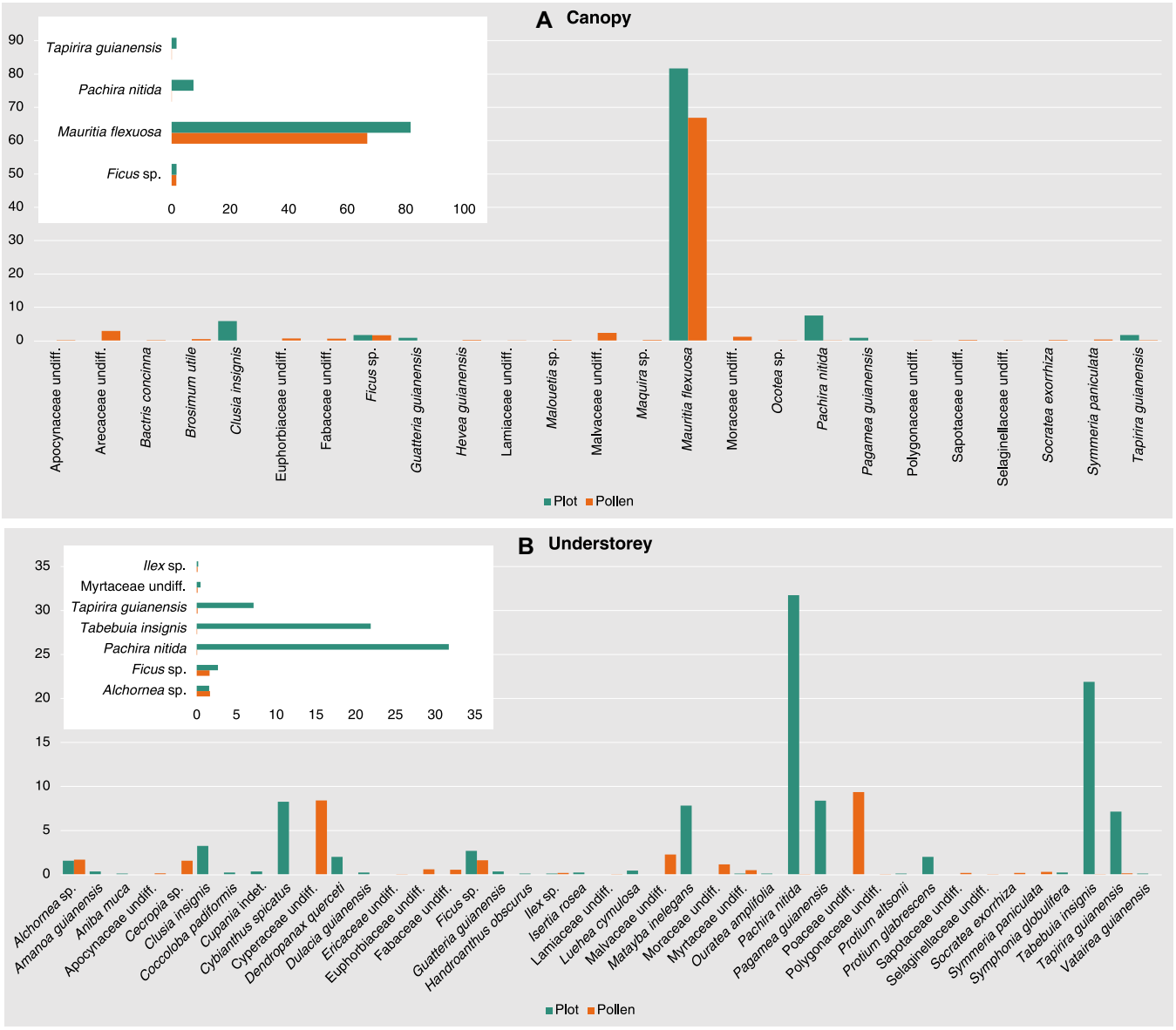

Figure 3. Comparison of taxon abundance in the vegetation plots with the abundance of pollen taxa in the surface sample. [Color figure can be viewed at wileyonlinelibrary.com]

and *Pagamea guianensis*. In the understorey, taxa that are abundant but not represented in the surface samples are *Cybianthus spicatus*, *Pagamea guianensis* and *Matayba inelegans*. In contrast, many taxa that are expressed palynologically are not present in the vegetation. Of these, abundant pollen taxa that are not recorded in the plot include *Hevea guianensis* (often found in wet conditions, e.g. seasonally flooded forest and in association with palm swamps; Honorio Coronado et al., 2021), *Bactris concinna* (common in palm swamps of the Peruvian Amazon; Kahn and Mejia, 1990) and *Symmeria paniculata* (typical of flooded forests; Ferreira and Stohlgren, 1999).

Four taxa identified in the surface samples are present in the plot among the trees and palms ≥10 cm DBH, and seven pollen taxa occur both in the surface samples and in the understorey vegetation. *Mauritia flexuosa* was the most abundant taxon among the large trees (82%) and *Mauritia*-t. pollen (the diameter of which confirms a high likelihood that it is derived from *Mauritia flexuosa*) represents 67% of the modern pollen assemblage and can thus be described as well represented in the surface samples. Further taxa that are represented with some fidelity in the surface samples are *Ficus* sp., present in both the canopy (1.67%) and the understorey (2.68%) with a palynological abundance of 1.6%; *Ilex* sp., present in the understorey (0.18%) and the surface samples (0.11%); and *Alchornea* sp., observed in the understorey at an abundance of 1.6% and a palynological abundance of 1.7%. Meanwhile, Myrtaceae are slightly under-represented, being present in the understorey at 0.5% abundance and in the surface samples at 0.1%. *Pachira nitida*, *Tapirira guianensis* and *Tabebuia insignis* are strongly under-represented – all three taxa are present in the understorey with abundances of 5–30% but do not reach 1% in the surface samples. In the canopy, *Pachira nitida* and *Tapirira guianensis* have an abundance of >10% and represent <1% of the pollen assemblage in the surface samples.

Sedimentology

The lowermost sedimentological unit (s-unit) of the core (570–550 cm, s-unit 1) is composed entirely of homogenous olive-grey clay (*Argilla steatodes*). Sediments between 550 and 500 cm (s-units 2–6) comprise a mix of clay-rich sediments and organic matter. The units between 500 and 367 cm

(s-units 7–13) are composed of herbaceous peat (*Turfa herbacea*) and woody peat (*Turfa lignosa*). The unit between 367 and 353 cm (s-unit 14) consists of clayey silts intermixed with peat. Between 353 and 182 cm (s-units 15–18), the material is composed of a homogeneous matrix of sub-fibrous peat. From 182 to 162 cm, s-units 19 and 20 are composed of herbaceous remains (*Detritus herbosus*) mixed with clayey material. Between 162 and 16 cm (s-units 21–23), the material is composed of very fibrous and loosely consolidated peat. From 16 to 0 cm (unit 24), insufficient material was recovered for palynological subsampling and analyses due to the unconsolidated nature of the substrate. The Troels-Smith (1955) description is summarized in Figure 4 and Appendix S3.

Chronology and accumulation rates

AMS radiocarbon dating (Table 1) shows a consistent pattern of older ages with greater depth, i.e. no reversals (Figure 4). The lowermost age determination, obtained at the base of the peat, is 3497 ± 37 a BP (median age 3750 cal a BP). Extrapolation suggests an estimated age of c. 4330 cal a BP for the base of the core, although the precise age is unknown considering the different lithology of the lowermost sedimentological unit. The average accumulation rate is 1.72 ± 0.83 mm a^{-1}.

Geochemistry

Magnetic susceptibility (*K*) reveals a pronounced difference between the lowermost 70 cm and the rest of the core (Figure 4). Between 550 and 570 cm, *K* is at its maximum, 30–40 × 10^{-6} SI units, indicating the presence of ferrimagnetic material in the sediments. As the content of inorganic sediments decreases between 500 and 550 cm, *K* values decrease to around 7–10 × 10^{-6} SI units. Between 500 and 200 cm, *K* values are less variable, ranging from −5 to 5 × 10^{-6} SI units. *K* values then return to between −1 and 1 × 10^{-6} SI units for the rest of the record.

C/N ratios (Figure 4) also show a pronounced difference between the base and the rest of the core. In the clay-rich unit between 560 and 570 cm, nitrogen is below the limit of detection. Between 500 and 560 cm, C/N increases rapidly during the transition from clay to organic-rich material, with C/N peaks

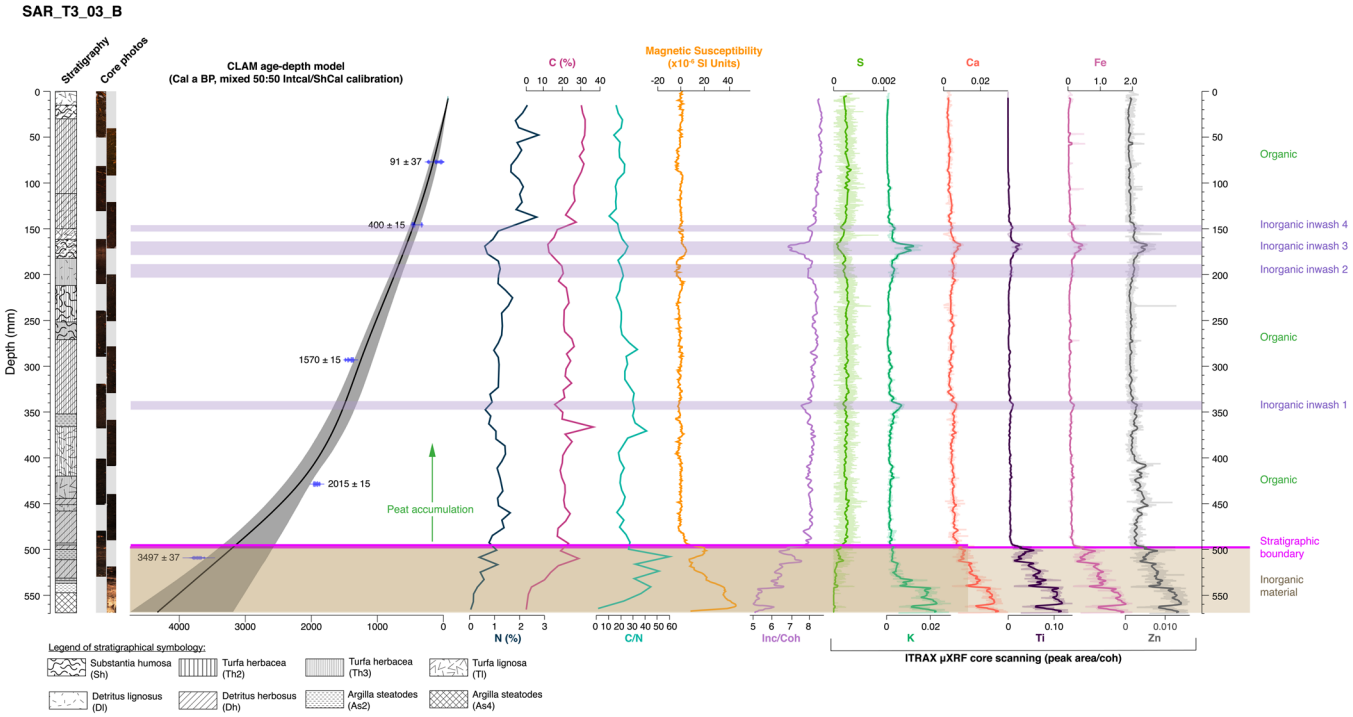

Figure 4. Summary graph for core SAR_T3_03_B showing: core stratigraphy; core photographs; age–depth model of SAR_T3_03_B developed using CLAM; nitrogen and carbon content; C/N ratios; magnetic susceptibility; the incoherent/coherent ratio; and selected elemental signals from the ITRAX core scanner. [Color figure can be viewed at wileyonlinelibrary.com]

Table 1. AMS radiocarbon dating results for the SAR_T3_03_B core. Dates were obtained from the NERC facility at East Kilbride [SUERC (Scottish Universities Environment Research Centre) and UCIAMS (Keck Carbon Cycle AMS Facility, University of California, Irvine, USA) prefixes]. Calibration was undertaken using the IntCal20/ShCal20 mixed curve.

Lab_ID	Depth (cm)	^{14}C enrichment (% modern ± 1σ)	Conventional radiocarbon age (years BP ± 1σ)	2σ calibrated age range (cal a BP)	Carbon content (%)
SUERC-93780	70–71	98.88 ± 0.45	91 ± 37	10–260	31.23
UCIAMS-251371	140–142	95.16 ± 0.15	400 ± 15	333–494	23.29
UCIAMS-251372	290–291	82.25 ± 0.15	1570 ± 15	1375–1513	18.40
UCIAMS-251373	428–429	77.81 ± 0.13	2015 ± 15	1891–1993	20.66
SUERC-93784	510–511	64.71 ± 0.30	3497 ± 37	3639–3863	11.47

between 45 and 60. C/N decreases slightly between 170 and 320 cm. A small peak in carbon content of 36% is observed at 368 cm, and dips in carbon and nitrogen are observed at 168 cm. From 140 cm to the top of the core, C/N is less variable with a range of 10–20.

Results from the μXRF core scanning (Figure 4) show an abundance of minerogenic elements at the base of the core, including potassium (K), calcium (Ca), titanium (Ti), iron (Fe), zirconium (Zr) and strontium (Sr) (indicative of inorganic material) and low values of the incoherent/coherent (inc/coh) ratios. The inc/coh ratio is frequently used as an indication of organic content, with a higher ratio indicating higher organic content (Longman et al., 2019). Between 500 and 570 cm, the inc/coh ratio shows a gradual increase. The abundances of sulphur (S) and manganese (Mn) are particularly low at these depths but rise from around 500 cm. Between 330 and 500 cm, the levels of S, Mn and the inc/coh ratio are high, while K, Ca, Ti, Fe, Zn, Sr and Zr decrease to low levels with minor fluctuations. Around 330 cm, coincident with a decrease in inc/coh ratio and a clay-rich layer observed in the stratigraphy, K, Ca, Ti, Fe, Zn, Sr and Zr all display a minor peak. Between 220 and 330 cm, an interval of low variability is observed, with high inc/coh ratios. Another phase of change in the geochemical signals is observed between 190 and 160 cm. This interval contains the highest peaks in Ca, K, Ti, Fe, Zn and Zr apart from the base of the core, and coincides with a decrease in the inc/coh ratio. Between 160 cm and the top of the record, the μXRF signal reveals a higher inc/coh ratio (>8) and a near absence of minerogenic material (K, Ca, Ti, Fe, Zn, Sr and Zr).

Palynological analysis

The pollen record (Figures 5–7) has a temporal resolution of 25–130 years. Concentrations of main sum pollen grains between 0 and 544 cm range from 17 600 to 806 000 grains cm^{-3} while in the clay-rich unit (560–570 cm) pollen concentrations are much lower, between 1300 and 32 000 grains cm^{-3}. Pollen preservation is good throughout the core, and indeterminable pollen grains make up less than 1% of the pollen count in all samples. Microcharcoal concentrations range from 500 to 200 000 fragments cm^{-3}, reaching a maximum at 528 cm. Palm phytoliths range from 0 to 80 000 phytoliths cm^{-3}, and occur throughout almost the entire record, reaching a maximum at 208 cm. The pollen diagram reveals distinct changes in pollen assemblage composition through the sequence, reflected in the five pollen assemblage zones determined through CONISS. The most pronounced changes in pollen assemblages are reported in Table 2.

Diameter measurements of *Mauritia flexuosa* and *Mauritiella armata* grains in samples from the SAR_T3_03_B core show grain diameters to vary from 20 to 60 μm with an average of 40 μm. Across the whole sequence, grains are split approximately evenly between the size classes, with 50.4% of grains measuring >40 μm and 49.6% measuring <40 μm, but their relative abundance varies stratigraphically. Smaller grains typical of *Mauritiella armata* are dominant at the bottom of the record in zone SAR-I (496–536 cm) and between the top of SAR-IV and the bottom of SAR-V (104–192 cm). Larger grains typical of *Mauritia flexuosa* are more abundant in zones SAR-II and SAR-III (264–424 cm), and in the uppermost part of zone SAR-V (16–64 cm).

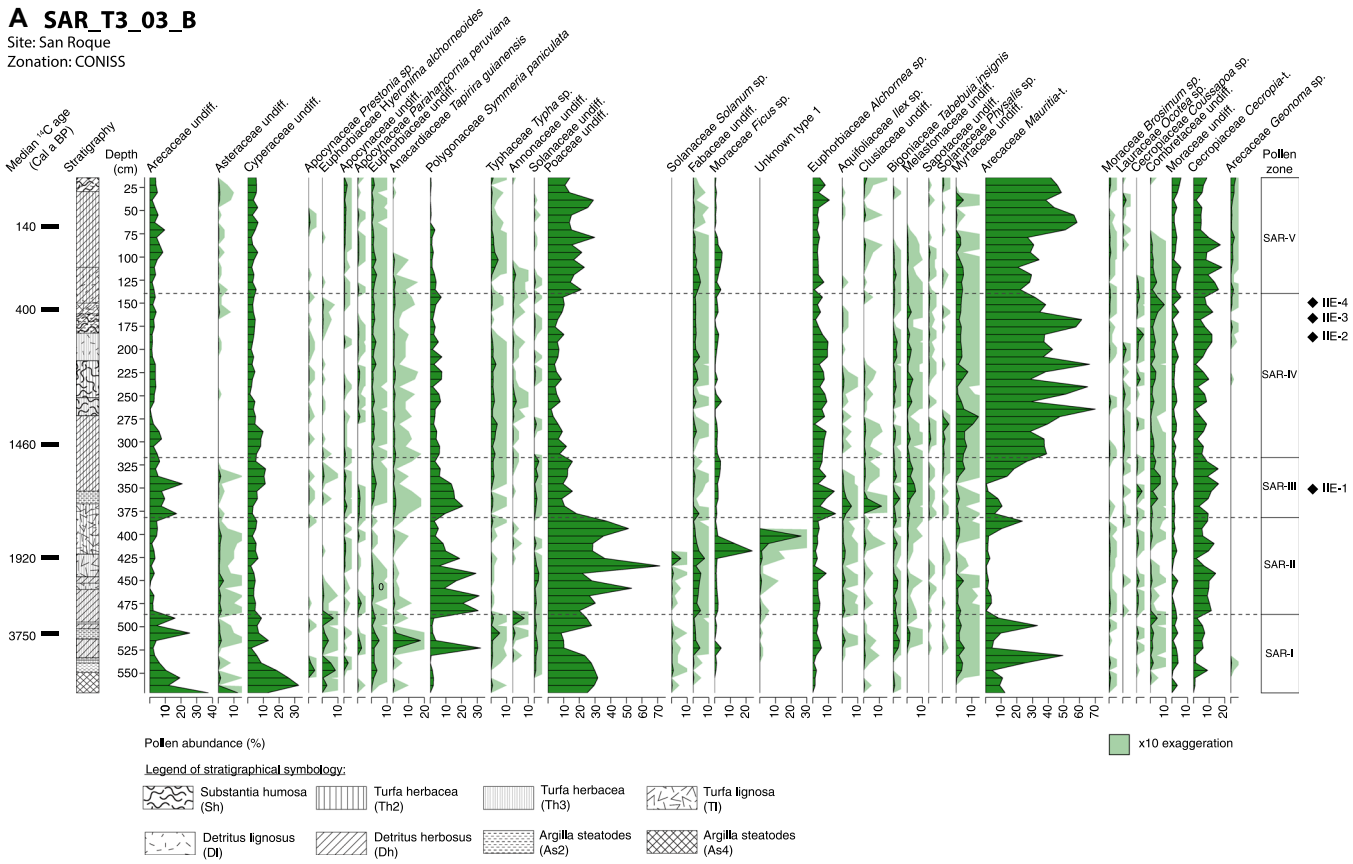

Figure 5. Percentage diagram (part A) showing abundance of major taxa (>5% abundance) in the SAR_T3_03_B record, plotted against depth. The Troels-Smith stratigraphic diagram and median radiocarbon ages (cal a BP) are plotted alongside land pollen abundance. The taxa have been ordered by the time at which maximum percentage abundance is reached, from left to right. Paler colours in the background indicate the ×10 exaggeration. Pollen assemblage zones are defined by Constrained Incremental Sum-of-Squares (CONISS). The diagram was developed using R. [Color figure can be viewed at wileyonlinelibrary.com]

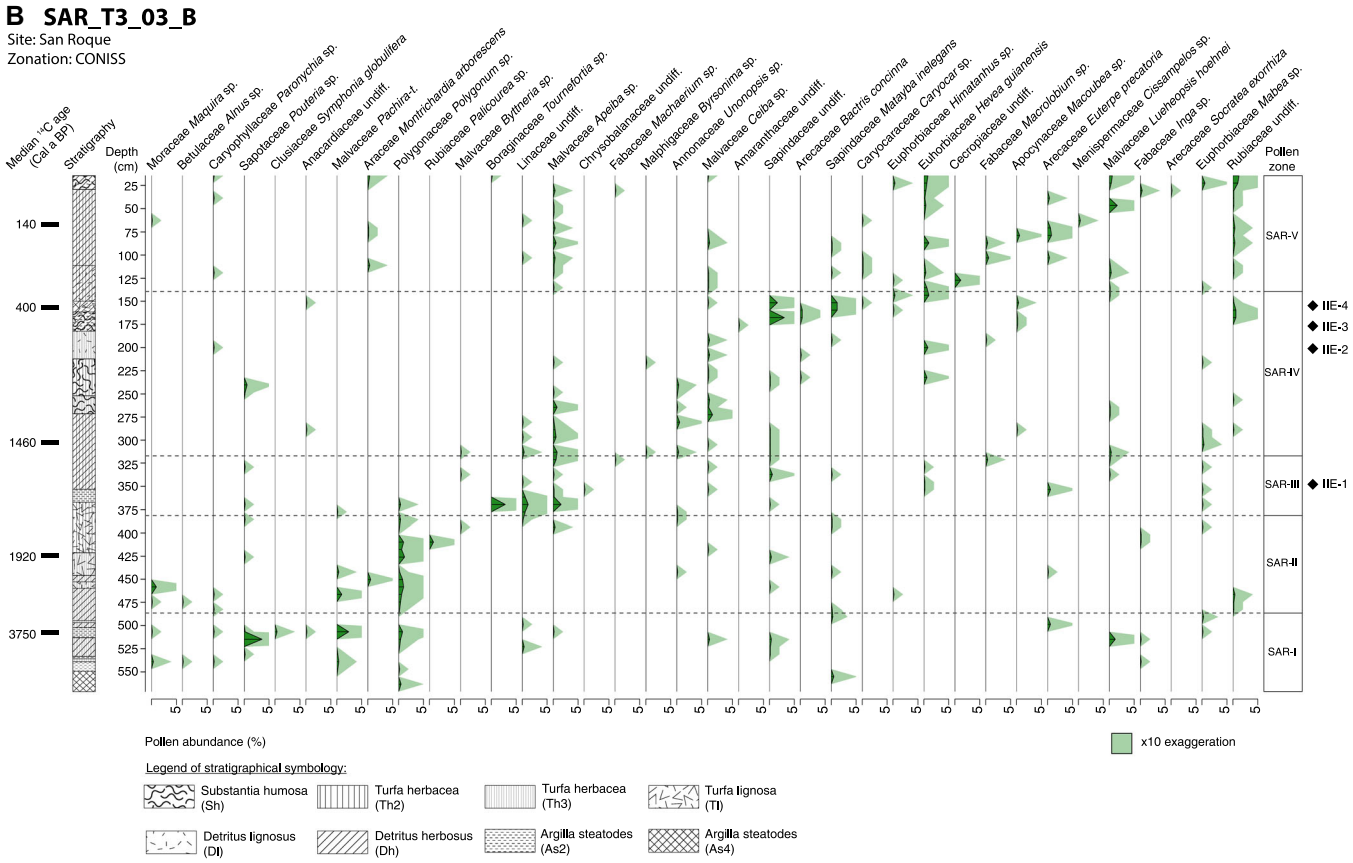

Figure 6. Percentage diagram (part B) showing abundance of the minor taxa (<5% abundance) in the SAR_T3_03_B record, plotted against depth. [Color figure can be viewed at wileyonlinelibrary.com]

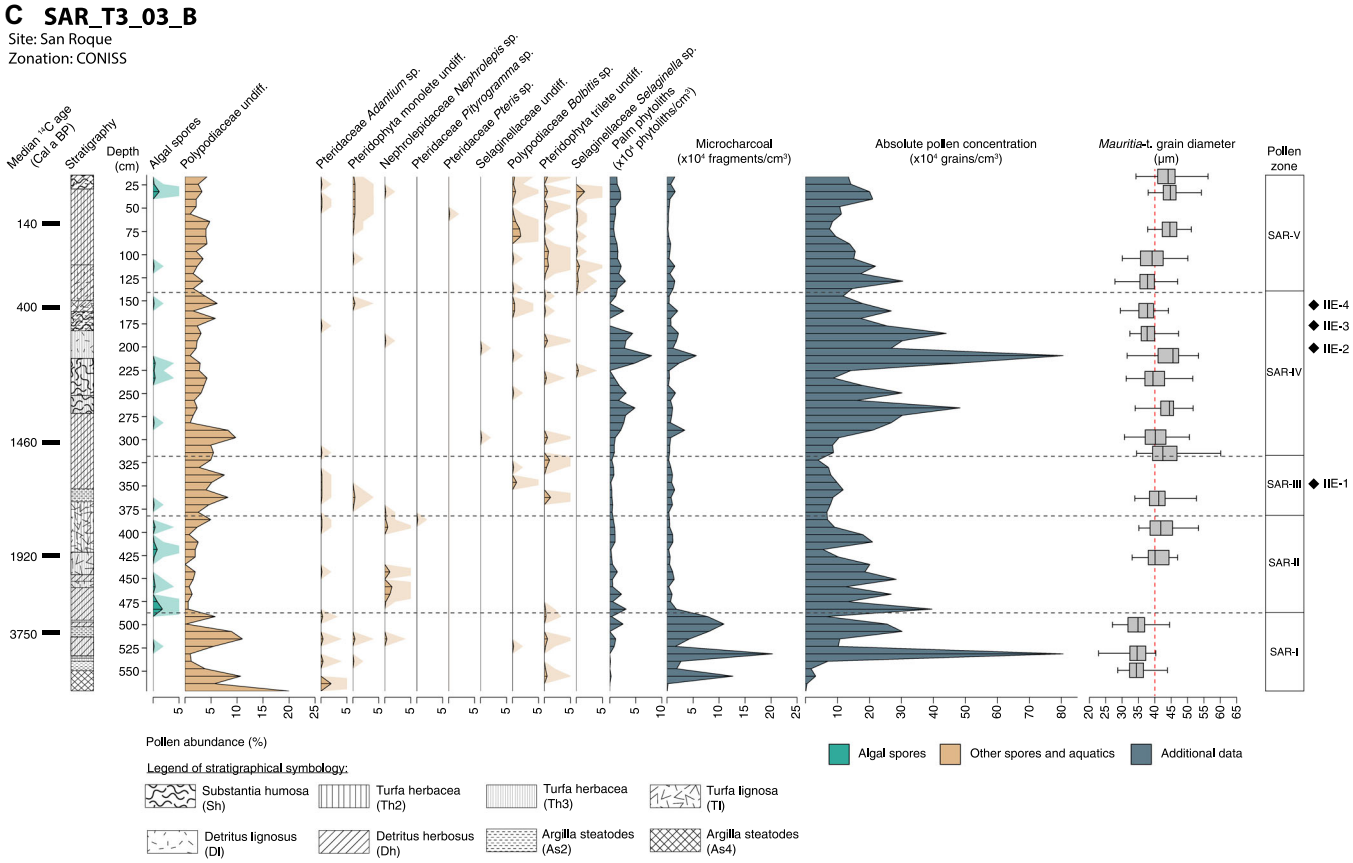

Figure 7. Percentage diagram (part C) showing abundance of spores, microcharcoal, phytoliths and absolute pollen concentrations in the SAR_T3_03_B record, plotted against depth, as well as total land pollen count and results from the *Mauritia*-t. measurements. [Color figure can be viewed at wileyonlinelibrary.com]

Table 2. Descriptions of pollen assemblage zones for SAR_T3_03_B.

Zone (depth)	Interpolated age (cal a BP)	Pollen zone description
SAR-V (140–16 cm)	460–present	Arecaceae undiff. increase slightly, although averaging <10%. Cyperaceae undiff. remain constant throughout the zone, while Poaceae undiff. increase to >20%. The levels of Euphorbiaceae undiff., *Symmeria paniculata*, *Typha* sp., Fabaceae undiff., *Ficus* sp., Myrtaceae undiff. and Combretacae undiff. all decrease steadily until becoming rare by the top of the record. *Alchornea* sp. is fairly constant, exhibiting a minor peak of >10% at 40 cm. *Cecropia*-t. fluctuates above and below 10% for the first half of the zone, until decreasing to <5% towards the end. *Mauritia*-t. increases from around 20% to more than 40%, dominating the assemblage. Minor taxa include: *Hevea guianensis, Euterpe precatoria, Lueheopsis hoehni, Socratea exorrhiza, Mabea* sp. and Rubiaceae undiff.
SAR-IV (316–140 cm)	1400–460	The levels of Arecaceae undiff., Cyperaceae undiff., *Symmeria paniculata* and Poaceae undiff. all decrease drastically to <10%, while *Mauritia*-t. becomes the most dominant taxon in the record averaging >40%, with a maximum peak of 66% occurring at 216 cm. Multiple peaks of *Mauritia*-t. occur, all exceeding 30%. *Mauritia*-t. and *Cecropia*-t. appear to alternate, although *Cecropia*-t. remains <10% throughout the entire zone. *Typha* sp. shows a slight increase, accompanied by a rise in Myrtaceae undiff., which peak to an abundance of 14% at 272 cm. *Tabebuia insignis*, Melastomaceae undiff., Moraceae undiff. (including *Ficus*), Euphorbiaceae undiff. and Combretaceae undiff. occur at steady levels below 10%. Minor taxa include: *Apeiba* sp., *Ceiba* sp., Sapindaceae undiff., *Matayba inelegans* and *Hevea guianensis*.
SAR-III (380–316 cm)	1770–1400	Arecaceae undiff. increase to >10%, accompanied by a rise in Cyperaceae undiff. and *Symmeria paniculata*. *Alchornea* sp. shows two peaks, with the highest in the record occurring at 376 cm (15%). A significant decrease in the abundance of Poaceae undiff. is observed, along with a fall in *Mauritia*-t., although this taxon experiences a sharp increase from <1% to 26% between 312 and 344 cm. *Ficus* sp., *Tabebuia insignis*, *Ilex* sp. and Melastomaceae undiff. undergo a slight increase in this zone, and Clusiaceae undiff. increase to >10% at 368 cm. Minor taxa include: *Tournefortia* sp, Linaceae undiff. and *Apeiba* sp.
SAR-II (484–380 cm)	2990–1770	Arecaceae undiff., Cyperaceae undiff. and *Mauritia*-t. show a pronounced decrease to <10%, while there is a significant rise in *Symmeria paniculata* (maximum peak of 31%) and Poaceae undiff. (maximum peak of 71%). The levels of *Cecropia*-t. also increase, with a peak of 14% at 440 cm. *Ficus* sp., *Solanum* sp. and Fabaceae undiff. also increase in abundance. Asteraceae remain present at very low levels, along with Euphorbiaceae undiff., Solanaceae undiff., *Alchornea* sp. and *Tabebuia insignis*. Minor taxa include: *Pachira*-t. and *Polygonum* sp. *Mauritia*-t. increases again to 24% at the end of the zone.
SAR-I (568–484 cm)	4330–2990	Arecaceae undiff. and Asteraceae undiff. first appear in this zone, with maximum abundances of 37% and 12% respectively. The levels of Cyperaceae undiff. and Poaceae undiff. are very high at the base of the record (>30%), decreasing to below 10% towards the top of the zone. *Mauritia*-t. is present with two distinct peaks of 49% at 528 cm and 33% at 496 cm. *Cecropia*-t. is present but at low levels of <10%. Other notable taxa occurring in this zone are *Hyeronima alchornoide*s, Euphorbiaceae undiff., *Typha* sp., Annonaceae undiff. and *Tapirira guianensis*, the last exhibiting a peak of 18% at 512 cm. *Symmeria paniculata* also has a localized peak of 32% at 520 cm. Minor taxa (<5%) include: *Pouteria* sp., *Maquira* sp. and *Pachira*-t.

Discussion

Palaeoenvironmental reconstruction

Zone SAR-I: 570–480 cm (c. 4330–2,990 cal a BP)

The clay-rich sediments at the bottom of the core are highly inorganic, as indicated by the low C%, N% and inc/coh ratio, and abundant Fe, Ti, Ca, K and Zn. These sediments are interpreted as fluvial input from white-water (i.e. sediment-laden) rivers (Croudace and Rothwell, 2016). The situation is comparable with the peatland sites San Jorge and Quistococha where similar clayey silts below the peat have been interpreted to indicate low-energy deposition environments, such as an overbank flood basin or oxbow lake (Roucoux et al., 2013; Lawson et al., 2014; Kelly et al., 2017, 2020).

Throughout the zone, the rise in inc/coh ratios gives a qualitative indication of the transition from low to high organic content (Kuhry and Vitt, 1996; Hatfield and Stoner, 2013; Aniceto et al., 2014; Longman et al., 2019). The increase in C/N ratios to ~30 indicates the presence of C_4 grasses and herbaceous vegetation – ratios of ≥12 are usually associated with C_3 vascular plants, whereas C_4 grasses typically have C/N ratios of ≥30 (Lamb et al., 2006). The gradually decreasing trend in Fe, Ti, K and Ca, elements related to fluvial input, and the significant rise in S, an element closely linked to organic matter, are interpreted as a progressive decrease in fluvial input and a change towards anaerobic organic decomposition (Croudace and Rothwell, 2016) – conditions related to the initiation of peat accumulation around 3180 cal a BP.

The high percentages of Cyperaceae undiff., Poaceae undiff., fern spores and algal spores (spheroidal, inaperturate with reticulate surface, ~12 µm in diameter; see Demske et al., 2013; Kelly, 2015) in the first half of this zone are consistent with the increase in C/N and inc/coh ratios. This assemblage is interpreted as the development of a herbaceous fen and/or herbaceous floating vegetation mats on open water – which are palynologically indistinguishable from each other (Roucoux et al., 2013; Kelly et al., 2017). This interval is also characterized by an abundance of *Cecropia*-t. (Roubik and Moreno, 1991; Colinvaux et al., 1988). Trees of the genus *Cecropia* are wind-pollinated, light-demanding pioneers which grow in disturbed areas, including open areas along riverbanks, and thus their abundance in the pollen spectrum supports the presence of open vegetation (such as that found by open water) at the coring site during this interval. Also

identified in this zone were Myrtaceae undiff., *Symmeria paniculata* and *Alchornea* sp. These taxa are mainly found in wetland habitats and seasonally flooded forests, and are present in the study area today. Therefore, their presence in this zone indicates that the floodwater level could have been high (>3 m) during this period (Lamotte, 1990; Parodi and Freitas, 1990; Kalliola et al., 1991; Campbell et al., 1992; Wittman et al., 2004; Roucoux et al., 2013). The interpretation of a flood-tolerant forest is also supported by measurements of *Mauritia*-t. grains in this zone: over 80% were smaller than 40 µm and therefore produced by *Mauritiella armata*. Its inferred abundance in the vegetation assemblage would be consistent with the occurrence of flood amplitudes higher than 1–2 m (Herrera and Urrego, 1996; Junk et al., 2015; Kelly et al., 2017). The vegetation at this time may have resembled seasonally flooded forest found close to the site today, dominated by *Mauritiella armata* and a diverse set of tree species including the Myrtaceae species *Eugenia florida* (census plot ROQ-05; Honorio Coronado et al., 2021).

The inorganic character of the sediment in this zone means that the pollen spectra may represent a large source area, the pollen having been carried to the site in flood water with the sediment and, since the depositional environment is likely to have been open water, also in air currents. Thus, the pollen assemblages in this zone are likely to represent vegetation growing some distance beyond the core site. Pollen taxa representing plants that are typical of palm swamps are present in this zone, including *Hyeronima alchornoides*, Euphorbiaceae undiff., Annonaceae undiff. and *Tapirira guianensis* (Draper et al., 2014, 2018), and taxa from pole forest ecosystems such as *Pachira*-t. (Honorio Coronado et al., 2021), indicating that these two forest types have been present in the landscape since the onset of peat development at the core site.

The high microcharcoal concentrations in this zone, ranging from 16 000 to 200 000 fragments cm^{-3}, may also be the result of long-distance transport. The small size (<20 µm) of the fragments is consistent with the fine-grained nature of the minerogenic sediments that characterize the base of the sequence. The concentrations in this record are high compared to other sites such as Quistococha, where the maximum is around 20 000 fragments cm^{-3} (Kelly et al., 2018). Based on the size, abundance and co-occurrence of microcharcoal with fine-grained sediments, we infer that the base of the San Roque record is likely to record fires occurring in the wider region rather than local to the site (Bush et al., 2015). Natural fires do not often occur in the ever-wet forests of NW Amazonia because of the constantly wet conditions (Mayle and Power, 2008; McMichael et al., 2012). Thus, when charcoal does occur in palaeoecological and archaeological records, it is usually attributed to anthropogenic burning (e.g. Behling and Hooghiemstra, 2000; Bush et al., 2000, 2004; McMichael et al., 2012). There is evidence of human settlements in the region during the period represented by this pollen zone. The archaeological studies of Rivas Panduro (2006) and Rivas Panduro, Oyuela-Caycedo, et al. (2006) showed human presence in the area around 2690–2350 cal a BP near the present-day lake of Quistococha, located about 150 km from our site (see also Kelly et al., 2017). An earlier study by Lathrap (1970), who studied evidence of human occupation along river channels in the Central Ucayali river basin, south of the PMFB, suggested that people may have occupied bluff areas in the floodplains of this region for the past 3500–4000 years. Other archaeological sites have been reported by Coomes et al. (2021) in the proximity of the San Roque peatland, although their age is unknown. Given the definitive archaeological evidence for human occupation in Amazonia by 10 000 cal a BP in Colombia, Bolivia and Brazil (Cavelier et al., 1995; Gnecco and Mora, 1997; Lombardo et al., 2013, 2020; Roosevelt, 2013; Watling et al., 2018; Maezumi et al., 2022), the possibility that humans have occupied this area of Amazonia during this period is very likely, even if archaeological evidence has not yet been found in the immediate vicinity of the core site. According to Denevan's (1996) 'bluff model' of human settlement in Amazonia, in which prehistoric communities (and their fires) were situated along the course of rivers, the attribution of anthropogenic origin to the abundant microcharcoal recorded in this fluvially dominated part of the sequence between 4330 and 3180 cal a BP seems plausible. Further analysis of micro- and macro-charcoal in peat cores from the PMFB could be a valuable way to further investigate past human activity in this region.

Zone SAR-II: 480–375 cm (c. 2990–1770 cal a BP)

This zone is marked by an increase in C%, N% and inc/coh ratios compared with the previous zone, indicating an increase in the organic content of the peat. Furthermore, *K* values and abundances of Fe, Ti, K and Ca are substantially lower, suggesting a reduction in the amount of sediment entering the site from white-water rivers. This could have been caused by a change in the position of the Marañón, perhaps due to avulsion or migration, taking the channel further away from the site (Davies-Vollum and Kraus, 2001).

However, an increase in *Symmeria paniculata* – a species tolerant of long flooding periods – and the presence of the flood-tolerant taxa *Alchornea* sp. and Myrtaceae undiff. are consistent with continued annual flooding at the site, even though sediment influx decreased. The rise in Poaceae undiff. and *Cecropia*-t., and the continued presence of Cyperaceae undiff., represent a continuation of open-canopy and herbaceous vegetation. These assemblages, characterized by herbaceous vegetation, riparian taxa and trees typical of flooded forests, are indicative of two vegetation types that may have been present at the same time in the area: (i) marginal fen or floating herbaceous mat vegetation and (ii) seasonally flooded forest. These pollen assemblages are similar to those of zone QT-2 from the peatland record at Quistococha, where herbaceous assemblages occurred alongside seasonally flooded forest taxa, during a period of prolonged and deep annual flooding (Roucoux et al., 2013). A phase of flood-tolerant trees and shrubs also occurs in palaeoecological records from the pole forest of Ollanta (Draper, 2015), indicating that early peatland succession phases are similar in three different peatland ecosystem types in the PMFB.

Mauritia-t. increases at the top of this zone. Over 60% of grains were larger than 40 µm, which indicates the presence of *Mauritia flexuosa*. As this taxon is not tolerant of prolonged or frequent flooding above 1.2 m deep (Junk et al., 2015; Flores Llampazo et al., 2022), its presence may be used to infer a reduction in flooding depth and frequency. The prevalence of Poaceae undiff. and the continued presence of Cyperaceae undiff. are indicative of herbaceous vegetation with an open canopy (Kelly et al., 2017). The presence of *Cecropia*-t. (maximum of 14% in this zone) could represent local presence of this genus – a light-demanding pioneer tree which is typically found in forest gaps and near open water, and which also tolerates flooding (Roubik and Moreno, 1991; Colinvaux et al., 2003; Weng et al., 2002). However, the parent trees of *Cecropia*-t. are often over-represented in the pollen signal, frequently contributing about 15–20% of the pollen rain even where it is not locally present (Bush and Colinvaux, 1988; Liu and Colinvaux, 1988; Lyons-Weiler, 1992; Weng et al., 2002). Thus, on the basis of the percentages encountered here, we can infer that *Cecropia* was certainly present in the region and could also have been present close to the core site though

perhaps only in small numbers, for example in open areas and along riverbanks.

Zone SAR-III: 375–312 cm (c. 1,770–1,400 cal a BP)

This interval is characterized by a minor rise in inorganic input as peat continued to accumulate, identified in the stratigraphy by higher clay content. The geochemical data show a short-lived decrease in C%, N%, inc/coh ratio and elemental S at 340–360 cm, and a synchronous rise in the elemental signal of K, Ca, Ti, Fe, Zn and Zr, labelled as Inorganic Inwash Event 1 (IIE-1; c. 1580–1520 cal a BP) in Figures 4 and 8. The geomorphologically active rivers of the PMFB can cause periods of relative stability and waterlogged conditions which promote the accumulation of peat, to alternate with phases of greater fluvial influence which can lead to increased minerogenic sedimentation in peatlands (Kalliola et al., 1992; Neller et al., 1992; Pärssinen et al., 1996; Lähteenoja et al., 2012). Thus, the geochemical changes observed in this zone are interpreted as a renewed increase in the arrival of sediment-laden flooding at the site, which could again have been caused by meandering or avulsion of the Marañón river.

The increase of *Symmeria paniculata*, Moraceae (including *Ficus* sp.), *Typha* sp., *Tabebuia insignis* and Euphorbiaceae (including *Alchornea* sp.) is interpreted as reflecting a change towards higher flood levels and duration compared to the previous zone. Furthermore, *Mauritia*-t. (dominated by grains >40 µm in diameter, and therefore indicative of the presence of *Mauritia flexuosa*) undergoes a significant decrease. Together these changes in the vegetation composition support the return of deeper (>1.2 m) seasonal flooding, inferred on the basis of renewed inorganic sediment influx.

Between 320 and 344 cm (c. 1540–1420 cal a BP), a second rise in *Mauritia*-t. is recorded. This is coeval with a period of low fluvial sediment inputs inferred on the basis of higher inc/coh ratios and consistently low abundance of elements indicative of inorganic sediment input. *Symmeria paniculata* decreases in this phase, and *Mauritia*-t. grain measurements for this part of the zone indicate a higher proportion of *Mauritia flexuosa* compared to *Mauritiella armata* supporting a return to lower flooding depth (Roucoux et al., 2013).

Zone SAR-IV: 312–136 cm (c. 1,400–460 cal a BP)

Between 312 and 210 cm (1380–830 cal a BP), there are minor fluctuations in the elemental abundance of K, Ca, Ti, Fe, Zn, Sr and Zr and inc/coh ratios. Throughout the zone, C/N appears to decrease steadily at a slow rate, from 20 to 15, possibly linked to a decrease in the amount of lignin input in the peat. In the µXRF elemental data, this pattern is represented by the recurrent rise in minerogenic elements particularly at c. 830–730 cal a BP (IIE-2), 690–610 cal a BP (IIE-3) and c. 560–510 cal a BP (IIE-4) (Figures 4 and 5), which are interpreted as sporadic episodes of enhanced input of fluvial sediment.

Lower overall minerogenic input and nutrient content compared with the previous zone, and a decrease in flooding conditions may have enabled an expansion of palm swamp taxa. *Mauritia*-t. increases rapidly in this zone, reaching abundances of ~30%. Measurements of *Mauritia*-t. grains indicate that pollen was predominantly derived from *Mauritia flexuosa*. This taxon probably occurred at low abundances, scattered in the landscape. In the modern pollen assemblage of the surface samples, local presence of scattered *Mauritia flexuosa* yielded pollen percentages of over 60%; *Mauritia flexuosa* pollen comprise >80% in *Mauritia flexuosa*-dominated

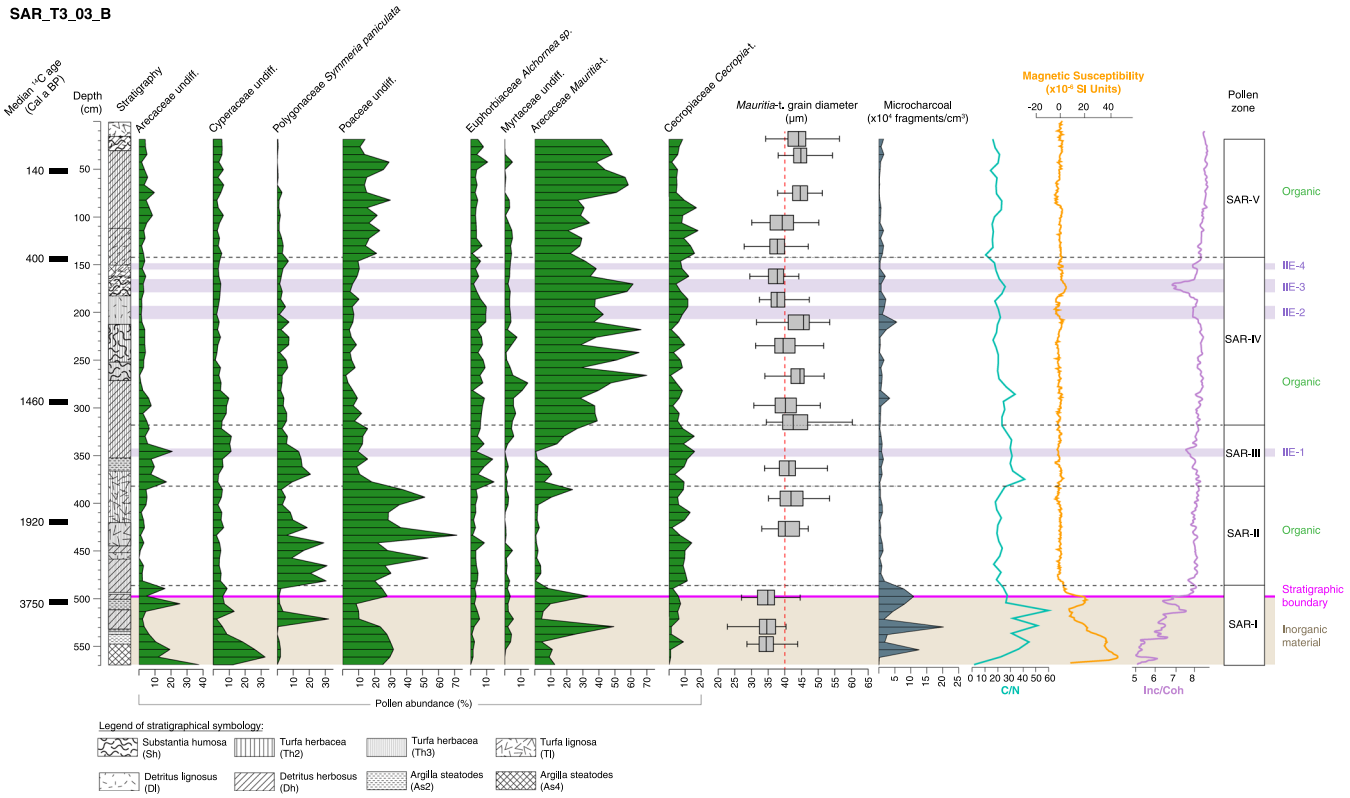

Figure 8. Summary diagram comparing changes in the key taxa used for the environmental interpretations, *Mauritia*-t. diameter measurements, microcharcoal, and the geochemical data including C/N ratios, magnetic susceptibility and the inc/coh ratio from the ITRAX core scanning, highlighting the timing of the Inorganic Inwash Events (IIEs). [Color figure can be viewed at wileyonlinelibrary.com]

palm swamps (e.g. Quistococha; Kelly et al., 2018). Other taxa indicative of peatland palm swamp vegetation such as *Tabebuia insignis*, Melastomaceae undiff. and Moraceae (including *Ficus* sp.) occur consistently with pollen percentages below 10%, while *Apeiba* sp., *Ceiba* sp., Sapindaceae undiff., *Matayba inelegans* and *Hevea guianensis* pollen are all below 5%, suggesting the presence of these taxa in the vicinity of the coring site but at low local abundance (Figures 4 and 5). The decrease of herbaceous vegetation including Poaceae undiff., Cyperaceae undiff., Polypodiaceae undiff. and, importantly, the flood-tolerant tree *Symmeria paniculata*, further supports the interpretation of a general reduction in flooding during this period albeit with episodic influxes of fluvial sediments.

The continuous presence of *Ficus* sp. in this zone and indeed throughout the record is notable since its flowers are cleistogamous (i.e. pollen remains inside a closed flower) and is therefore expected to be poorly represented in the pollen record. However, as shown in our investigation on vegetation representation in the modern pollen signal, *Ficus* sp. tends to be well represented in the pollen assemblage and is a common part of the vegetation. Therefore, an abundance of *Ficus* sp. in the pollen record can be interpreted to represent trees of this taxon growing close to the core site, consistent with the direct local contribution of this pollen via gravity processes.

A short-lived phase of increased flooding by sediment-laden waters is inferred between 190 and 160 cm, designated here as IIE-3 (c. 690–610 cal a BP), characterized by a decrease in the inc/coh ratio and a sharp rise in all elements related to minerogenic sediments (K, Ca, Ti, Fe, Zn, Sr, Zr). This phase represents the highest input of inorganic sediments since before the onset of peat accumulation. In the pollen record, this phase coincides with an increase in Myrtaceae undiff. and Poaceae undiff. Although a lag in the response of palm swamp vegetation is observed, *Mauritia*-t. declines steadily between 170 and 140 cm, over an interval of 300 years. During this period, a high proportion of *Mauritia*-t. grains (>70%) measured less than 40 µm, indicative of the presence of *Mauritiella armata*. Together, these results point to an interval with higher flood levels.

Zone SAR-V: 136–16 cm (c. 460 cal a BP–present day)

Low levels of the minerogenic elements Fe, Ti, Ca, K, Sr, Zn and Zr in this zone indicate low fluvial sediment influx. The reduction in fluvial sediment input in this zone suggests that the regional component of the pollen signal is likely to be smaller, and thus more representative of the local changes at the coring site. The C/N ratio is consistently within the range of 10–20 indicating the presence of terrestrial C_3 vascular plants (Lamb et al., 2006).

The pollen assemblage of this zone comprises a higher abundance of *Mauritia*-t. (60%), which is characterized almost entirely by pollen larger than 40 µm and therefore likely to have been produced by *Mauritia flexuosa*. This abundance is similar to the results for modern pollen rain, in which *Mauritia*-t. made up 67% of the assemblage in the surface samples and represented over 80% of the current tree assemblage. This could suggest that *Mauritia flexuosa* occurred in similar numbers to the present day. The low percentages of *Symmeria paniculata*, *Typha* sp. and Myrtaceae undiff. indicate that deep seasonal flooding ceased at this point (Roucoux et al., 2013). Meanwhile, the presence of pollen types identifiable to *Hevea guianensis*, *Euterpe precatoria*, *Lueheopsis hoehni* and *Socratea exorrhiza* indicate the first establishment of peatland palm swamp vegetation in the vicinity of the coring site. These species are characteristic of peatland palm swamps in the region today and no other species in the same genera are present, supporting the specific attribution.

The prevalence of Poaceae undiff. and Cyperaceae undiff. and the continued presence of *Cecropia*-t. indicate that, even though *Mauritia*-t. and other palm swamp taxa have become more abundant, the canopy remained relatively open allowing light-demanding vegetation to persist (Kelly et al., 2017). The pollen assemblage in the upper part of this zone is similar to those of the surface samples. We observe a high abundance of herbaceous taxa (Poaceae undiff. and Cyperaceae undiff.) and *Mauritia*-t., and a signal from several less abundant taxa typical of flooded forests (*Alchornea* sp., *Symmeria paniculata*) as well as taxa commonly found in palm swamp environments (*Socratea exorrhiza*, *Hevea guianensis*, *Ficus* sp.). However, one notable difference from the present-day vegetation and the pollen assemblage of the surface samples is the complete absence of *Pachira*-t. grains in the pollen assemblage of this zone even though this taxon is present in the vegetation today. Two explanations may be considered: (i) as shown by our modern vegetation–pollen comparison and earlier work by others, *Pachira* sp. is not a prolific pollen producer and its pollen is transported only very short distances, mainly by bats (Colinvaux et al., 2003), and therefore even if it were growing locally, it may have not be represented in the pollen record; or (ii2) *Pachira* sp. may not have been present in the vegetation here yet, and has only started to grow in the understorey near the core site more recently (indeed the top 16 cm of the core were not retrieved so the last few hundred years are not recorded). The recent arrival of *Pachira* sp. in the vegetation can be compared to the findings in the pollen records from the peatland pole forests of San Jorge and Ollanta (Kelly et al., 2017), where it appears in the uppermost pollen samples, representing the last c. 200 years.

Influence of flooding variability on peatland development and vegetation change

The pollen record from the San Roque peatland shows changes in the vegetation assemblage spanning the past c. 4330 years and the geochemical record shows changes in the fluvial sediment supply (Figure 8), thus providing a picture of the influence of the river inundation regime on the vegetation.

The most pronounced fluvial influence is observed at the time before peat accumulation. Lateral channel migration, in this case the movement of the Marañón river, and the increasing distance of the basin from the river, may have isolated the site from the main channel, a pattern previously observed in studies in the region (Salo et al., 1986; Kalliola et al., 1992; Puhakka et al., 1992). This change promoted the establishment of pioneer species such as *Cecropia*-t. (Foster, 1980; Lamotte, 1990; Kalliola et al., 1991, 1992), and the development of herbaceous vegetation communities including floating mats (Kalliola et al., 1992; Puhakka et al., 1992), leading to the onset of peat accumulation. A similar successional pattern has been inferred from other records from the PMFB (Roucoux et al., 2013; Lawson et al., 2014; Kelly et al., 2017, 2020). At Quistococha, Kelly et al. (2018) showed that the site developed after the abandonment of an active meander of the Amazon river, and that regular flooding brought clayey silts into the basin between 4500 and 2400 cal a BP, after which peat began to accumulate. Then, in the low-lying areas where floodwater became trapped, autogenic processes led to the expansion of *Cecropia*-dominated vegetation and abundant herbaceous taxa including Poaceae undiff. and Cyperaceae undiff. (Roucoux et al., 2013; Kelly et al., 2017; Swindles et al., 2018).

At the core site of San Roque, peat accumulation and compaction enabled the herbaceous fen-like community to expand towards the centre of the basin. Diverse flood-tolerant trees and shrubs began to establish, including *Alchornea* sp., *Symmeria paniculata* and Myrtaceae undiff., occurring after the development of the herbaceous taxa and before the establishment of *Mauritia flexuosa*. Despite the contrast in geographical setting, there may be some similarities with the processes observed in North American peatland sites, where floating mats expand laterally, promoting peat formation and the gradual replacement of herbaceous taxa by rooted taxa until ultimately mature forests develop (Kratz and DeWitt, 1986; Futyma and Miller, 1986). In our record, however, phases characterized by a higher abundance of flood-tolerant taxa (e.g. in zones SAR-II and SAR-IV) are interpreted as diversions of the ecological succession due to changes in floodwater levels. Similar intervals were observed in the records from Quistococha and San Jorge. After the establishment of the palm swamp at Quistococha and a herbaceous fen with scattered palms at San Jorge, the records show a transition to a *tahuampa* forest (flooded by black-water rivers for 3–6 months of the year) and an open fen, respectively (Roucoux et al., 2013; Kelly et al., 2017). The prolonged presence or reoccurrence of flood-tolerant vegetation phases at the sites of San Roque, Quistococha and San Jorge may be related to the fluctuations in the flooding regime as inferred from independent evidence. In contrast to Quistococha and San Jorge, however, the data from San Roque point towards the occurrence of several changes in flooding conditions as the peat accumulated. There is evidence that these intermittent periods of higher flood levels and increased supply of sediment-laden, nutrient-rich floodwater promoted the establishment of flood-tolerant species and repeatedly inhibited the development of a palm swamp.

These findings are consistent with previous observations by Lähteenoja and Page (2011) who showed, using ^{14}C-dated geochemical records, that the minerogenic open peatlands of Nueva Allianza and Maquía were higher in nutrients (predominantly Ca, Mg, Mn, Fe, K and S) throughout their developmental history and more frequently prone to inundation compared to other (forested) peatland vegetation types in the PMFB. A tentative picture is therefore emerging of a key role for flooding impacts in promoting the long-term maintenance of open peatlands.

A particularly notable interval of inorganic fluvial input in the SAR T3_03_B record is IIE-3 (c. 690–610 cal a BP) since the timing of this event coincides with the period known as the Medieval Climate Anomaly (MCA), occurring around 1230–1390 CE (1100–600 cal a BP; Mann, 2002; Lüning et al., 2019). Evidence from Ecuador, from the pollen records of Anañgucocha (1000 m asl; Frost, 1988) and Limoncocha (230 m asl), Lake Agrio (330 m asl) and Lake Santa Cecilia (330 m asl; Colinvaux et al., 1988) supports a climate during the MCA in the Amazon that was predominantly wetter than the present day. Ledru et al. (2013) inferred similar conditions for this time based on the pollen record from the peatland site of Papallacta (3815 m asl), suggesting a warm and moist climate over the Ecuadorian Andes. The transport of inorganic sediments in white-water rivers during such a period of increased wetness may explain the increase in flooding and the related influx of inorganic material at our site. However, this pattern of increased wetness during the time of the MCA is not found in all records from NW Amazonia. For example, Weng et al. (2002) showed that the vegetation assemblages in their records from the northern lowlands of Ecuador (Maxus-1 and Maxus-4) reflected a warmer and drier climate than before the MCA. Liu and Colinvaux (1988) suggested a similar interpretation to the above studies for climate during the MCA using the record from Lake Kumpak, in the southern lowlands of Ecuador. Furthermore, Stansell et al. (2013) inferred from the %Ca record from Queshquecocha in the Peruvian Andes (4260 m asl) that glaciers in the Andean Ice Sheet were retreating at this time, thus providing further supporting evidence for a drier and warmer climate. Although the results from SAR_T3_03_B are consistent with higher flooding at the site during the MCA, this may be either the result of greater water discharge in the rivers caused by higher precipitation, or an increase in meltwater carried by white-water rivers from the Andes to the PMFB, or both processes combined. Thus, it is difficult to assign a specific driver to the patterns observed in the SAR_T3_03_B record because climate, fluvial and autogenic processes are linked and are likely to have all contributed collectively to hydrological conditions and vegetation change together. The heterogeneity of Amazonia's response to suprarregional climatic influences, including climatic changes on the scale of the MCA, but also shorter-term cycles such as ENSO, make it challenging to identify a single explanation for the changes observed in records from this region. Future work on the interconnections between climate, rivers and vegetation in this region is becoming increasingly necessary if we want to better interpret pollen records and evaluate the sensitivity of Amazonian peatlands to external drivers.

In summary, it appears that the ecology, dynamics and ecological succession of the open peatland of San Roque was influenced by rivers more strongly and, importantly, more frequently than other peatland sites studied previously in the PMFB. This is likely to reflect the proximity to the Marañon river, characteristics of the floodwater and/or topographic elevation of the peatland site. The persistence over millennia of open herbaceous peatland phases could be at least partly due to deflection of succession by intervals of deeper and more frequent flooding by sediment-laden waters. The greater influence of flooding at the peatland core site of San Roque has created unsuitable conditions for the full development of peatland palm swamp or pole forest. The frequent input of nutrients during floods may have promoted the growth of taxa better adapted to higher flood levels and more nutrient-rich soils, thereby causing the prevalence of open peatland vegetation with interspecific competition between flood-tolerant vegetation and palm swamp taxa through time.

Conclusion

The palynological and geochemical records from the SAR_T3_03_B core show changes in vegetation and flooding variability in the open peatland of San Roque over the past c. 4330 years. The pollen record has enabled the identification of distinctive phases of ecological succession in peatland vegetation, beginning with floating mat and herbaceous communities at the time of peat initiation, transitioning towards flood-tolerant forest and finally developing into an 'open' peatland characterized by a mixture of palm swamp and pole forest taxa with scattered *Mauritia flexuosa*. While this overall successional pattern is consistent with other peatlands in the region and the Northern Hemisphere, periods at San Roque which could be interpreted as incipient peatland palm swamp expansion appear to have been interrupted on several occasions by shifts to deep and prolonged flooding correlating with inorganic influxes within the peat. By creating more limiting conditions for palm swamp taxa and encouraging taxa better adapted to higher flood levels and more nutrient-rich soils, the hydrological conditions at the site appear to have hindered the growth of *Mauritia flexuosa* and other palm swamp taxa for thousands of years. Conditions seem to have become more suitable for the establishment of peatland palm swamp taxa only in the past few centuries, also permitting the

recent establishment of peatland pole forest taxa (i.e. *Pachira* sp.) in the vicinity even more recently.

The potential for climatic and human influence has also been considered, but disentangling their signal from fluvial and flooding variability remains speculative at this stage. While there was no clear botanical indication of human presence detected in the pollen, a continuous record of microcharcoal was found, possibly related to a continuous background signal derived from anthropogenic burning in the fluvial catchment. The high concentrations found within the clayey sediments at the base of the SAR_T3_03_B record could represent long-distance fluvial input of charcoal which may result from anthropogenic burning of vegetation in the wider region.

Responses to climate changes in the wider Amazonian region were tentatively identified in the record, specifically an increase in flood-tolerant taxa and minerogenic elements around 1100–600 cal a BP (IIE-3) correlated with the MCA. However, disentangling climate, fluvial and autogenic processes remains a difficult task because these drivers are linked and contribute to change in flooding regime and vegetation collectively.

In conclusion, this record contributes to our understanding of peatland formation and vegetation change in the PMFB by showing that flooding variability is a key driver of peatland development, influencing the type of vegetation that developed over long periods. Although the present-day peatland of San Roque has been classified as an 'open' peatland through remote sensing, it has undergone a series of ecological succession phases and is likely to continue evolving. This dynamism is significant because it means that as the peatland continues to accumulate and becomes more forested with tree taxa, it is likely to store increasing quantities of below-ground carbon. However, the recent trajectory of change at this site (towards a situation with more trees) could well be diverted back to a more open state in future if or when the flooding regime changes again, under future scenarios of climate change or with continued migrations of the Marañon river.

Acknowledgements and funding. We gratefully acknowledge the financial support of the School of Environment, Education and Development (SEED) at the University of Manchester for funding a PhD studentship to D.S., and from NERC to I.T.L. and K.H.R. (grant code NE/R000751/1). Thanks also to the Quaternary Research Association for granting the New Research Workers' award, which made it possible to travel to Peru for fieldwork. We are grateful to the colleagues from the Instituto de Investigaciones de la Amazonia Peruana (IIAP), Nallaret Dávila, Julio Irarica, Julio Grandez and James Reyna who provided invaluable assistance during fieldwork, and to the staff at the Geography Laboratories at the University of Manchester for the assistance provided during the laboratory work. Many thanks to NERC for awarding two rounds of radiocarbon dating under the NERC UK Radiocarbon Award (allocation numbers 2204.1019 and 2349.0321), and to Pauline Gulliver for assisting us throughout the application process. Special thanks to Dr. Frank Mayle for providing some of the modern reference material to the team at the University of St Andrews which was used for the pollen identification. We also acknowledge support from an NERC Knowledge Exchange Fellowship (NE/V018760/1) to E.N.H.C., a Leverhulme Trust research grant (RPG-2018-306) to K.H.R., and funding from Charles University (PRIMUS/23/SCI/013) to A.H.

Data availability statement

The data that support the findings of this study are available from the corresponding author upon reasonable request.

Supporting information

Additional supporting information can be found in the online version of this article.

Abbreviations. AGC, above-ground carbon; BGC, below-ground carbon; CHNS, carbon, nitrogen, hydrogen, sulphur (mode selected for elemental analyser); CONISS, Constrained Incremental Sum-of-Squares; DBH, diameter at breast height; ENSO, El Niño Southern Oscillation; IIE, Inorganic Inwash Event; ITCZ, Intertropical Convergence Zone; *K*, volumetric magnetic susceptibility; MCA, Medieval Climate Anomaly; PMFB, Pastaza–Marañón Foreland Basin; ROQ, Roque (i.e. San Roque), prefix for vegetation plot identification codes; s-unit, sedimentological unit; SOC, soil organic carbon; SPT, sodium polytungstate; μXRF, micro X-ray fluorescence.

References

Absy, M.L. (1979) A palynological study of Holocene sediment in the Amazon Basin. PhD Thesis, University of Amsterdam, Netherlands.

Aniceto, K., Moreira-Turcq, P., Cordeiro, R.C., Fraizy, P., Quintana, I. & Turcq, B. (2014) Holocene paleohydrology of Quistococha Lake (Peru) in the upper Amazon Basin: Influence on carbon accumulation. *Palaeogeography, Palaeoclimatology, Palaeoecology*, 415, 165–174.

Behling, H. & Hooghiemstra, H. (2000) Holocene Amazon rainforest–savanna dynamics and climatic implications: high-resolution pollen record from Laguna Loma Linda in eastern Colombia. *Journal of Quaternary Science*, 15(7), 687–695.

Birks, H.J.B. (1996) Contributions of Quaternary palaeoecology to nature conservation. *Journal of vegetation science*, 7(1), 89–98.

Bishop, T. (2021) *Using Itrax Data in R*. Available at: https://tombishop1.github.io/itraxBook/ (accessed: 12/08/2021).

Blaauw, M. (2010) Methods and code for "classical" age-modelling of radiocarbon sequences. *Quaternary Geochronology*, 5(5), 512–518.

Bodmer, R., Mayor, P., Antunez, M., Chota, K., Fang, T., Puertas, P. et al. (2018) Major shifts in Amazon wildlife populations from recent intensification of floods and drought. *Conservation Biology*, 32(2), 333–344.

Brown, A.D. (2010) Pollen analysis and planted ancient woodland restoration strategies: a case study from the Wentwood, southeast Wales, UK. *Vegetation History and Archaeobotany*, 19(2), 79–90.

Burn, M.J. & Mayle, F.E. (2008) Palynological differentiation between genera of the Moraceae family and implications for Amazonian palaeoecology. *Review of Palaeobotany and Palynology*, 149(3–4), 187–201.

Bush, M., De Oliveira, P., Colinvaux, P., Miller, M. & Moreno, J. (2004) Amazonian paleoecological histories: One hill, three watersheds. *Palaeogeography, Palaeoclimatology, Palaeoecology*, 214(4), 359–393.

Bush, M.B. & Colinvaux, P.A. (1988) A 7000-year pollen record from the Amazon lowlands, Ecuador. *Vegetatio*, 76(3), 141–154.

Bush, M.B., McMichael, C.H., Piperno, D.R., Silman, M.R., Barlow, J., Peres, C.A. et al. (2015) Anthropogenic influence on Amazonian forests in pre-history: an ecological perspective. *Journal of Biogeography*, 42(12), 2277–2288.

Bush, M.B., Miller, M.C., De Oliveira, P.E. & Colinvaux, P.A. (2000) Two histories of environmental change and human disturbance in eastern lowland Amazonia. *The Holocene*, 10(5), 543–553.

Campbell, D.G., Stone, J.L. & Rosas, A. (1992) A comparison of the phytosociology and dynamics of three floodplain (Várzea) forests of known ages, Rio Juruá, western Brazilian Amazon. *Botanical Journal of the Linnean Society*, 108(3), 213–237.

Campbell, J.F.E., Fletcher, W.J., Hughes, P.D. & Shuttleworth, E.L. (2016) A comparison of pollen extraction methods confirms dense-media separation as a reliable method of pollen preparation. *Journal of Quaternary Science*, 31(6), 631–640.

Cargille, J.J. (2008) Immersion oil and the microscope. Available at: https://biochimie.umontreal.ca/wp-content/uploads/sites/37/2012/08/Immersion_Oil_and_the_Microscope.pdf (accessed 04 August 2021).

Cavelier, I., Rodríguez, C., Herrera, L.F., Morcote, G. & Mora, S. (1995) No solo de caza vive el hombre: ocupación del bosque amazónico, Holoceno temprano. Ámbito y ocupaciones tempranas de la América Tropical. pp. 27–44.

Charman, D. (2002) *Peatlands and environmental change*. John Wiley and Sons Ltd.

Colinvaux, P.A., Frost, M., Frost, I., Liu, K.B. & Steinitz-Kannan, M. (1988) Three pollen diagrams of forest disturbance in the western Amazon basin. *Review of Palaeobotany and Palynology*, 55(1-3), 73–81.

Colinvaux, P.A., De Oliveira, P.E. & Moreno, E. (2003) *Amazon: pollen manual and atlas*. CRC Press.

Coomes, O.T., Rivas Panduro, S., Abizaid, C. & Takasaki, Y. (2021) Geolocation of unpublished archaeological sites in the Peruvian Amazon. *Scientific Data*, 8(1), 290.

Cox, P.M., Betts, R.A., Collins, M., Harris, P.P., Huntingford, C. & Jones, C.D. (2004) Amazonian forest dieback under climate-carbon cycle projections for the 21st century. *Theoretical and applied climatology*, 78(1), 137–156.

Croudace, I.W. & Rothwell, R.G. (2016) *Micro-XRF Studies of Sediment Cores: Applications of a non-destructive tool for the environmental sciences*, vol. 17. Springer

Dargie, G.C., Lewis, S.L., Lawson, I.T., Mitchard, E.T.A., Page, S.E., Bocko, Y.E. et al. (2017) Age, extent and carbon storage of the central Congo Basin peatland complex. *Nature*, 542(7639), 86–90.

Davies-Vollum, K.S. & Kraus, M.J. (2001) A relationship between alluvial backswamps and avulsion cycles: An example from the Willwood Formation of the Bighorn Basin Wyoming. *Sedimentary Geology*, 140(3–4), 235–249.

Dearing, J. (1999) Magnetic susceptibility. In: Walden, J., Oldfield, F. & Smith, J. (Eds.) *Environmental Magnetism: A Practical Guide*, 6. London, UK: Quaternary Research Association Technical Guide No. 6. pp. 35–62.

Demske, D., Tarasov, P.E. & Nakagawa, T. (2013) Atlas of pollen, spores and further non-pollen palynomorphs recorded in the glacial-interglacial late Quaternary sediments of Lake Suigetsu, central Japan. *Quaternary International*, 290-291, 164–238.

Denevan, W.M. (1996) A bluff model of riverine settlement in prehistoric Amazonia. *Annals of the Association of American Geographers*, 86, 654–681.

Dias Saba, M. (2007) Morfologia Polínica de Malvaceae: Implicaciones Taxonômicas e Filogeneticas. Unpublished PhD Thesis, Universidad estadual de Feira de Santana.

Djamali, M. & Cilleros, K. (2020) Statistically significant minimum pollen count in Quaternary pollen analysis; the case of pollen-rich lake sediments. *Review of Palaeobotany and Palynology*, 275, 104156.

Draper, F.C. (2015) Carbon storage and floristic dynamics in Peruvian peatland ecosystems. Unpublished PhD thesis, University of Leeds, UK.

Draper, F.C., Honorio Coronado, E.N., Roucoux, K.H., Lawson, I.T., A. Pitman, N.C., A. Fine, P.V. et al. (2018) Peatland forests are the least diverse tree communities documented in Amazonia, but contribute to high regional beta-diversity. *Ecography*, 41(8), 1256–1269.

Draper, F.C., Roucoux, K.H., Lawson, I.T., Mitchard, E.T.A., Honorio Coronado, E.N., Lähteenoja, O. et al. (2014) The distribution and amount of carbon in the largest peatland complex in Amazonia. *Environmental Research Letters*, 9(12), 124017.

Dumont, J.F. & Garcia, F. (1991) Active subsidence controlled by basement structures in the Maranon Basin of northeastern Peru. IAHS Publication. *International Association of Hydrological Sciences*, 200, 343–350.

Endress, B.A., Horn, C.M. & Gilmore, M.P. (2013) Mauritia flexuosa palm swamps: Composition, structure and implications for conservation and management. *Forest Ecology and Management*, 302, 346–353.

Faegri, F. & Iversen, J. (1989) *Textbook of Pollen Analysis*, 4th Edition. Chichester, UK: John Wiley and Sons.

Ferreira, L.V. & Stohlgren, T.J. (1999) Effects of river level fluctuation on plant species richness, diversity, and distribution in a floodplain forest in Central Amazonia. *Oecologia*, 120(4), 582–587.

Flores Llampazo, G., Honorio Coronado, E.N., del Aguila-Pasquel, J., Cordova Oroche, C.J., Díaz Narvaez, A., Reyna Huaymacari, J. et al. (2022) The presence of peat and variation in tree species composition are under different hydrological controls in Amazonian wetland forests. *Hydrological Processes*, 36(9), e14690.

Foster, R.B. (1980) Heterogeneity and disturbance in tropical vegetation. In: Soule, M.E. & Wilcox, B.A. (Eds.) *Conservation biology: an evolutionary–ecological perspective*. Massachusetts: Sinauer Associates. pp. 75–92.

Freitas Alvarado, L., Otárola Acevedo, E., Del Castillo Torres, D., Linares Bensimón, C., Martínez Dávila, P. & Malca Salas, G.A. (2006) Servicios ambientales de almacenamiento y secuestro de carbono del ecosistema aguajal en la Reserva Nacional Pacaya Samiria, Loreto-Perú.

Frost, I. (1988) A Holocene sedimentary record from Anangucocha in the Ecuadorian Amazon. *Ecology*, 69(1), 66–73.

Futyma, R.P. & Miller, N.G. (1986) Stratigraphy and genesis of the Lake Sixteen peatland, northern Michigan. *Canadian Journal of Botany*, 64(12), 3008–3019.

Gilmore, M.P., Endress, B.A. & Horn, C.M. (2013) The socio-cultural importance of Mauritia flexuosa palm swamps (aguajales) and implications for multi-use management in two Maijuna communities of the Peruvian Amazon. *Journal of Ethnobiology and Ethnomedicine*, 9, 29–52.

Gloor, M., Barichivich, J., Ziv, G., Brienen, R., Schöngart, J., Peylin, P. et al. (2015) Recent Amazon climate as background for possible ongoing and future changes of Amazon humid forests. *Global Biogeochemical Cycles*, 29(9), 1384–1399.

Gloor, M., Brienen, R.J.W., Galbraith, D., Feldpausch, T.R., Schöngart, J., Guyot, J.L. et al. (2013) Intensification of the Amazon hydrological cycle over the last two decades. *Geophysical Research Letters*, 40(9), 1729–1733.

Gnecco, C. & Mora, S. (1997) Late Pleistocene/early Holocene tropical forest occupations at San Isidro and Peña Roja, Colombia. *Antiquity*, 71(273), 683–690.

Grimm, E.C. (1987) CONISS: a FORTRAN 77 program for stratigraphically constrained cluster analysis by the method of incremental sum of squares. *Computers & Geosciences*, 13(1), 13–35.

Hastie, A., Honorio Coronado, E.N., Reyna, J., Mitchard, E.T.A., Åkesson, C.M., Baker, T.R. et al. (2022) Risks to carbon storage from land-use change revealed by peat thickness maps of Peru. *Nature Geoscience*, 15, 369–374.

Hatfield, R.G. & Stoner, J.S. (2013) Paleoceanography, Physical And Chemical Proxies | Magnetic Proxies and Susceptibility. In: Elias S.A. & Mock C.J. (Eds.), *Encyclopedia of Quaternary Science*. pp. 884–898.

Herrera, L.F. & Urrego, L.E. (1996) *Pollen atlas of useful and cultivated plants in the Colombian Amazon region. Studies on the Colombian Amazonia*, vol. XI. Bogotá, Colombia: Tropenbos.

Hogg, A.G., Heaton, T.J., Hua, Q., Palmer, J.G., Turney, C.S., Southon, J. et al. (2020) SHCal20 Southern Hemisphere Calibration, 0-55 000 Years cal bp. *Radiocarbon*, 62(4), 759–778.

Honorio Coronado, E.N., Hastie, A., Reyna, J., Flores, G., Grández, J., Lähteenoja, O. et al. (2021) Intensive field sampling increases the known extent of carbon-rich Amazonian peatland pole forests. *Environmental Research Letters*, 16(7), 074048.

Honorio Coronado, E.N., Vega-Arenas, J.E. & Corrales-Medina, M.N. (2015) Diversidad, estructura y carbono de los bosques aluviales del noreste. *Folia Amazónica*, 24(1), 55–70.

Huisman, S.N., Raczka, M.F. & McMichael, C.N.H. (2018) Palm phytoliths of mid-elevation Andean forests. *Frontiers in Ecology and Evolution*, 6(193), 1–8.

Juggins, S. (2020) *Package "rioja" – Analysis of Quaternary Science Data*. The Comprehensive R Archive Network.

Junk, W.J., Wittmann, F., Schöngart, J. & Piedade, M.T.F. (2015) A classification of the major habitats of Amazonian black-water river floodplains and a comparison with their white-water counterparts. *Wetlands Ecology and Management*, 23(4), 677–693.

Kahn, F. & Mejia, K. (1990) Palm communities in wetland forest ecosystems of Peruvian Amazonia. *Forest Ecology and Management*, 33–34(C), 169–179.

Kalliola, R., Puhakka, M., Salo, J., Tuomisto, H. & Ruokolainen, K. (1991) The dynamics, distribution and classification of swamp vegetation in Peruvian Amazonia. *Finnish Zoological and Botanical Publishing Board*, 28(3), 225–239.

Kalliola, R., Salo, J., Puhakka, M., Rajasilta, M., Häme, T., Neller, R.J. et al. (1992) Upper Amazon channel migration: implications for vegetation perturbance and succession using bitemporal lands at MSS images. *Naturwissenschaften*, 79(2), 75–79.

Kelly, T.J. (2015) *The long-term development of peatlands in Peruvian Amazonia*. Unpublished PhD thesis, University of Leeds.

Kelly, T.J., Lawson, I.T., Roucoux, K.H., Baker, T.R. & Honorio Coronado, E.N. (2020) Patterns and drivers of development in a west Amazonian peatland during the late Holocene. *Quaternary Science Reviews*, 230, 106168.

Kelly, T.J., Lawson, I.T., Roucoux, K.H., Baker, T.R., Honorio-Coronado, E.N., Jones, T.D. et al. (2018) Continuous human presence without extensive reductions in forest cover over the past 2500 years in an aseasonal Amazonian rainforest. *Journal of Quaternary Science*, 33(4), 369–379.

Kelly, T.J., Lawson, I.T., Roucoux, K.H., Baker, T.R., Jones, T.D. & Sanderson, N.K. (2017) The vegetation history of an Amazonian domed peatland. *Palaeogeography, Palaeoclimatology, Palaeoecology*, 468, 129–141.

Kratz, T.K. & DeWitt, C.B. (1986) Internal factors controlling peatland-lake ecosystem development. *Ecology*, 67(1), 100–107.

Kuhry, P. & Vitt, D.H. (1996) Fossil carbon/nitrogen ratios as a measure of peat decomposition. *Ecology*, 77(1), 271–275.

Lähteenoja, O., Reátegui, Y.R., Räsänen, M., Torres, D.D.C., Oinonen, M. & Page, S. (2012) The large Amazonian peatland carbon sink in the subsiding Pastaza-Marañón foreland basin, Peru. *Global Change Biology*, 18(1), 164–178.

Lähteenoja, O., Ruokolainen, K., Schulman, L. & Oinonen, M. (2009a) Amazonian peatlands: an ignored C sink and potential source. *Global Change Biology*, 15(9), 2311–2320.

Lähteenoja, O., Ruokolainen, K., Schulman, L. & Oinonen, M. (2009b) Amazonian floodplains harbour minerotrophic and ombrotrophic peatlands. *Catena*, 79(2), 140–145.

Lamb, A.L., Wilson, G.P. & Leng, M.J. (2006) A review of coastal palaeoclimate and relative sea-level reconstructions using $\delta^{13}C$ and C/N ratios in organic material. *Earth-Science Reviews*, 75(1–4), 29–57.

Lamotte, S. (1990) Fluvial dynamics and succession in the lower Ucayali River basin, Peruvian Amazonia. *Forest Ecology and Management*, 33–34I, 141–156.

Lathrap, D.W. (1970) *The Upper Amazon*. London: Thames & Hudson.

Lawson, I.T., Jones, T.D., Kelly, T.J., Coronado, E.N.H. & Roucoux, K.H. (2014) The Geochemistry of Amazonian Peats. *Wetlands*, 34(5), 905–915.

Lähteenoja, O.and Page, S. (2011) High diversity of tropical peatland ecosystem types in the Pastaza-Marañón basin, Peruvian Amazonia. *Journal of Geophysical Research: Biogeosciences*, 116(2), 1–14.

Ledru, M.P., Jomelli, V., Samaniego, P., Vuille, M., Hidalgo, S., Herrera, M. et al. (2013) The Medieval Climate Anomaly and the Little Ice Age in the eastern Ecuadorian Andes. *Climate of the Past*, 9(1), 307–321.

Liu, K.B. & Colinvaux, P.A. (1988) A 5200-Year History of Amazon Rain Forest. *Journal of Biogeography*, 15(2), 231–248.

Lombardo, U., Iriarte, J., Hilbert, L., Ruiz-Pérez, J., Capriles, J.M. & Veit, H. (2020) Early Holocene crop cultivation and landscape modification in Amazonia. *Nature*, 581(7807), 190–193.

Lombardo, U., Szabo, K., Capriles, J.M., May, J.H., Amelung, W., Hutterer, R. et al. (2013) Early and middle Holocene hunter-gatherer occupations in Western Amazonia: The hidden shell middens. *PLoS One*, 8(8), e72746.

Longman, J., Veres, D. & Wennrich, V. (2019) Utilisation of XRF core scanning on peat and other highly organic sediments. *Quaternary International*, 514, 85–96.

López Gonzales, M., Hergou'lc'h, K., Angulo Núñez, Ó., Baker, T., Chimner, R., del Águila Pasquel, J. et al. (2020) *Qué sabemos sobre las turberas peruanas?* Vol. 208. CIFOR.

López Parodi, J. & Freitas, D. (1990) Geographical aspects of forested wetlands in the lower Ucayali, Peruvian Amazonia. *Forest Ecology and Management*, 33-34, 157–168.

Lüning, S., Gałka, M., Bamonte, F.P., Rodríguez, F.G. & Vahrenholt, F. (2019) The medieval climate anomaly in South America. *Quaternary International*, 508, 70–87.

Lyons-Weiler, J. (1992) *Palynological analysis of a Holocene sedimentary sequence from the western Amazon basin*. Unpublished MS dissertation, Ohio State University.

Maezumi, S.Y., Elliott, S., Robinson, M., Betancourt, C.J., Gregorio de Souza, J., Alves, D. et al. (2022) Legacies of Indigenous land use and cultural burning in the Bolivian Amazon rainforest ecotone. *Philosophical Transactions of the Royal Society, B: Biological Sciences*, 377(1849), 20200499.

Malhi, Y., Aragão, L.E.O.C., Galbraith, D., Huntingford, C., Fisher, R., Zelazowski, P. et al. (2009) Exploring the likelihood and mechanism of a climate-change-induced dieback of the Amazon rainforest. *Proceedings of the National Academy of Sciences*, 106(49), 20610–20615.

Mann, M.E. (2002) Little ice age. *Encyclopedia of global environmental change*, 1, 504–509.

Marengo, J.A. & Espinoza, J.C. (2016) Extreme seasonal droughts and floods in Amazonia: causes, trends and impacts. *International Journal of Climatology*, 36(3), 1033–1050.

Marengo, J.A., Nobre, C.A., Tomasella, J., Cardoso, M.F. & Oyama, M.D. (2008) Hydro-climatic and ecological behaviour of the drought of Amazonia in 2005. *Philosophical Transactions of the Royal Society, B: Biological Sciences*, 363(1498), 1773–1778.

Marengo, J.A., Tomasella, J. & Uvo, C.R. (1998) Trends in streamflow and rainfall in tropical South America: Amazonia, eastern Brazil, and northwestern Peru. *Journal of Geophysical Research: Atmospheres*, 103(D2), 1775–1783.

Mayle, F.E. & Power, M.J. (2008) Impact of a drier Early–Mid-Holocene climate upon Amazonian forests. *Philosophical Transactions of the Royal Society, B: Biological Sciences*, 363(1498), 1829–1838.

McMichael, C.H., Piperno, D.R., Bush, M.B., Silman, M.R., Zimmerman, A.R., Raczka, M.F. et al. (2012) Sparse pre-Columbian human habitation in western Amazonia. *Science*, 336(6087), 1429–1431.

Mertes, L.A.K. (1997) Documentation and significance of the perirheic zone on inundated floodplains. *Water Resources Research*, 33, 1749–1762.

Moore, P.D., Webb, J.A. & Collinson, M.E. (1991) *Pollen Analysis*. London, UK: Blackwell.

Neller, R.J., Salo, J.S. & Räsänen, M.E. (1992) On the formation of blocked valley lakes by channel avulsion in Upper Amazon foreland basins. *Zeitschrift für Geomorphologie*, 36, 401–411.

Page, S.E., Rieley, J.O. & Banks, C.J. (2011) Global and Regional Importance of the Tropical Peatland Carbon Pool. *Global Change Biology*, 17(2), 798–818.

Palacios, J., Zárate, R., Torres-Reyna, G., Denux, J.P., Maco-García, J.T., Gallardo, G.P. et al. (2016) Mapeo De Los Bosques Tipo Varillal Utilizando Imágenes De Satélite Rapideye En La Provincia Maynas, Loreto, Perú. *Folia Amazónica*, 25(1), 25–36.

Pärssinen, M.H., Salo, J.S. & Räsänen, M.E. (1996) River flood- plain relocations and the abandonment of Aborigine settlements in the Upper Amazon Basin: A historical case study of San Miguel de Cunibos at the Middle Ucayali River. *Geoarchaeology*, 11(4), 345–359.

Patterson, W.A., Edwards, K.J. & Maguire, D.J. (1987) Microscopic Charcoal as a Fossil Indicator of Fire. *Quaternary Science Reviews*, 6(1), 3–23.

Pennington, R.T., Lavin, M., Prado, D.E., Pendry, C.A., Pell, S.K. & Butterworth, C.A. (2004) Historical climate change and speciation: neotropical seasonally dry forest plants show patterns of both Tertiary and Quaternary diversification. *Philosophical Transactions of the Royal Society of London. Series B: Biological Sciences*, 359(1443), 515–538.

Phillips, O.L., Baker, T.R., Brienen, R. & Feldpausch, T.R. (2010) Field manual for plot establishment and remeasurement. Available at: http://www.geog.leeds.ac.uk/projects/rainfor/ (accessed August 2023).

Piotrowska, N., Blaauw, M., Mauquoy, D. & Chambers, F.M. (2011) Constructing deposition chronologies for peat deposits using radiocarbon dating. *Mires and Peat*, 7(10), 1–14.

Puhakka, M., Kalliola, R., Rajasilta, M. & Salo, J. (1992) River types, site evolution and successional vegetation patterns in Peruvian Amazonia. *Journal of Biogeography*, 19(6), 651–665.

R Core Team (2021). *R: A language and environment for statistical computing*. R Foundation for Statistical Computing, Vienna, Austria.

Räsänen, M., Neller, R., Salo, J. & Jungner, H. (1992) Recent and ancient fluvial deposition systems in the Amazonian foreland basin, Peru. *Geological Magazine*, 129(3), 293–306.

Rasband, W.S. (2018). *ImageJ*. U.S. National Institutes of Health, Bethesda, Maryland, USA.

Reimer, P.J., Austin, W.E.N., Bard, E., Bayliss, A., Blackwell, P.G., Bronk Ramsey, C. et al. (2020) The IntCal20 Northern Hemisphere radiocarbon age calibration curve (0–55 cal kBP). *Radiocarbon*, 62(4), 725–757.

Ribeiro, K., Pacheco, F.S., Ferreira, J.W., de Sousa-Neto, E.R., Hastie, A., Krieger Filho, G.C. et al. (2021) Tropical peatlands and their contribution to the global carbon cycle and climate change. *Global Change Biology*, 27(3), 489–505.

Rivas Panduro, S. (2006) *Proyecto de Investigacion: Excavaciones Arqueologicas en Quistococha, Loreto-Amazonia Peruana*. Lima, Peru: Instituto Nacional de Cultura del Peru.

Rivas Panduro, S., Oyuela-Caycedo, A. & Zimmerman, A. (2006) Informe preliminar sobre los hallazgos en el sitio arqueologico de Quistococha, Amazonia Peruana. In: Bol. Estudios Amazónicos. Universidad Nacional Mayor de San Marcos. pp. 79–97.

Roosevelt, A.C. (2013) The Amazon and the Anthropocene: 13 000 years of human influence in a tropical rainforest. *Anthropocene*, 4, 69–87.

Roubik, D.W. & Moreno, J.E. (1991) Pollen and spores of Barro Colorado Island. *Missouri Botanical Garden*, 36, 270.

Roucoux, K.H., Lawson, I.T., Baker, T.R., Del Castillo Torres, D., Draper, F.C., Lähteenoja, O. et al. (2017) Threats to intact tropical peatlands and opportunities for their conservation. *Conservation Biology*, 31(6), 1283–1292.

Roucoux, K.H., Lawson, I.T., Jones, T.D., Baker, T.R., Coronado, E.N.H., Gosling, W.D. et al. (2013) Vegetation development in an Amazonian peatland. *Palaeogeography, Palaeoclimatology, Palaeoecology*, 374, 242–255.

Salo, J., Kalliola, R., Häkkinen, I., Mäkinen, Y., Niemelä, P., Puhakka, M. et al. (1986) River dynamics and the diversity of Amazon lowland forest. *Nature*, 322(6076), 254–258.

Schulman, L., Ruokolainen, K. & Tuomisto, H. (1999) Parameters for global ecosystem models. *Nature*, 399(6736), 535–536.

Schulz, C., Martín Brañas, M., Núñez Pérez, C., Del Aguila Villacorta, M., Laurie, N., Lawson, I.T. et al. (2019) Peatland and wetland ecosystems in Peruvian Amazonia: indigenous classifications and perspectives. *Ecology and Society*, 24(2), 1–17.

Seubert, E. (1996) Root anatomy of palms II. Calamoideae. *Feddes Repertorium*, 107(1–2), 43–59.

Stansell, N.D., Rodbell, D.T., Abbott, M.B. & Mark, B.G. (2013) Proglacial lake sediment records of Holocene climate change in the western Cordillera of Peru. *Quaternary Science Reviews*, 70, 1–14.

Swindles, G.T., Morris, P.J., Whitney, B., Galloway, J.M., Gałka, M., Gallego-Sala, A. et al. (2018) Ecosystem state shifts during long-term development of an Amazonian peatland. *Global Change Biology*, 24(2), 738–757.

Tafur Rengifo, L. (2001) Distrito Iquitos, Capital Iquitos. *Kanatoari, Iquitos*, 131–152.

Troels-Smith, J. (1955) Karakterisering af løse jordarter. Danmarks Geologiske Undersøgelse IV. *Række*, 3(10), 1–73.

Walker, D. (1970) Direction and rate in some British post-glacial hydroseres. In: Walker, D. & West, R.G., (Eds.) *Studies in the Vegetational History of the British Isles*. Cambridge, UK: Cambridge University Press. pp. 117–139.

Watling, J., Shock, M.P., Mongeló, G.Z., Almeida, F.O., Kater, T., De Oliveira, P.E. et al. (2018) Direct archaeological evidence for Southwestern Amazonia as an early plant domestication and food production centre. *PLoS One*, 13(7), e0199868.

Weng, C., Bush, M.B. & Athens, J.S. (2002) Holocene climate change and hydrarch succession in lowland Amazonian Ecuador. *Review of Palaeobotany and Palynology*, 120(1–2), 73–90.

Wittmann, F., Junk, W.J. & Piedade, M.T.F. (2004) The várzea forests in Amazonia: flooding and the highly dynamic geomorphology interact with natural forest succession. *Forest Ecology and Management*, 196(2–3), 199–212.

Wüst, R.A.J., Bustin, R.M. & Lavkulich, L.M. (2003) New classification systems for tropical organic-rich deposits based on studies of the Tasek Bera Basin, Malaysia. *Catena*, 53(2), 133–163.

